UNIVERSITY OF THE AEGEAN – SCHOOL OF ENVIRONMENT – DEPARTMENT OF MARINE SCIENCES

FRESHWATER BUDGET VARIABILITY OF THE BLACK SEA AND ITS RELATION TO THE MEAN SEA LEVEL

Mosiou Kyriaki

THESIS

Supervisor: Tragou Eleni-Anthi

Mytilene, February 2019

THESIS

of the Department of Marine Sciences graduate

Kyriaki Mosiou

STUDY SUBJECT:

FRESHWATER BUDGET VARIABILITY OF THE BLACK SEA AND ITS RELATION TO THE MEAN SEA LEVEL

Thesis Committee	Signatures
Tragou Eleni-Anthi **Supervisor**	
Zervakis Vasilis	
Velegrakis Antonis	

Acknowledgements

I would sincerely like to thank my thesis supervisor, Prof. Eleni-Anthi Tragou of the Department of Marine Sciences at University of the Aegean, for the invaluable guidance concerning the realization of this thesis and for lighting my spark of interest for physical oceanography.

I would also like to thank the rest of the thesis committee, Prof. Vasilis Zervakis and Prof. Antonis Velegrakis of the Department of Marine Sciences at University of the Aegean, for their purposeful comments on the improvement of the document in question.

Additionally, I would like to express my appreciation towards all the professors of the Department of Marine Sciences that I had the pleasure to attend a class with, since each and one of them have done their bit in establishing the foundations of my scientific understanding.

I would like to give special thanks to the doctoral candidate Stamatis Petalas of the Department of Marine Sciences for kindly providing me key results from his personal work, and the doctoral candidate Giannis Mamoutos of the Department of Marine Sciences for providing valuable assistance on technical matters regarding this thesis.

Finally, I would like to thank all of my friends for their encouragement and most of all my family for their emotional and financial support.

Abstract

The variability of the freshwater budget of the Black Sea and its relation with the mean sea level has been investigated, employing an array of products from different sources to succeed the study. The highly novel mass concentration estimations from GRACE have played an important role as the connecting agent between the freshwater budget variability and the mean sea level of the Black Sea. Utilizing specific methodology, the results have demonstrated a positive influence of the freshwater influx fluctuations to the variability of the basin's water mass and consequently its mean sea level. In particular, the riverine contribution clearly influences the mass of Black Sea, and shapes the upper layer flux in the Bosphorus Strait.

Περίληψη

Στη παρούσα εργασία εξετάστηκε η μεταβλητότητα του ισοζυγίου του γλυκού νερού της Μαύρης Θάλασσας και η σχέση αυτού με τη μέση θαλάσσια στάθμη, χρησιμοποιώντας μια σειρά δεδομένων από διαφορετικές πηγές. Τα καινοτόμα δεδομένα της συγκέντρωσης μάζας από την αποστολή GRACE έπαιξαν σημαντικό ρόλο συνδέοντας το ισοζύγιο του γλυκού νερού με τη μέση θαλάσσια στάθμη της Μαύρης Θάλασσας. Ακολουθώντας συγκεκριμένη μεθοδολογία, τα αποτελέσματα αυτής της εργασίας δείχνουν μια θετική επιρροή των διακυμάνσεων του ισοζυγίου του γλυκού νερού στην μεταβλητότητα της μάζας του νερού της εν λόγω λεκάνης και ως συνέπεια της μέσης θαλάσσιας στάθμης της. Συγκεκριμένα, η ποτάμια συνεισφορά επηρεάζει σημαντικά τη μάζα της λεκάνης της Μαύρης Θάλασσας, και διαμορφώνει το ανώτερο στρώμα ροής στο στενό του Βοσπόρου.

Table of Contents

1. Introduction

The most basic understanding of the sea level is the analogy of water in a bathtub, the water height rises when liquid is added and falls when liquid is subtracted (Kopp *et al.,* 2015). In reality, sea level change is by far more complex given that it happens in a rotating self-gravitating planet, which has a visco-elastic deforming mantle, plus wind stresses and buoyancy fluxes at the surface of the water (Kopp *et al.,* 2015). Depending on the nature of the forcing, sea level change has a very wide spatial and temporal range, from a few millimeters to a meter or from hours to centuries (Rhein *et al.,* 2013). In addition, both climate variables and dynamical processes are reflected upon the sea level (Rhein *et al.,* 2013). With this information into account, the clarification of sea level change is of utmost importance.

Primarily, there are two available methods to measure this natural occurrence. The first one that appeared two centuries ago is the employment of tide gauges, which in reality measure the combination of volume expansion/contraction and the vertical land movement (VLM, later described as isostatic rebound) (Rhein *et al.,* 2013). The second method is achieved through satellite altimetry, which measures the distance from the satellite to the ocean surface at a given instant and expresses it via sea surface height (SSH). Then, the sea level anomaly (SLA) can be acquired through the subtraction of a reference ellipsoid (e.g. geoid) from the SSH (Leuliette *et al*., 2004). In other words, tide gauges measure relative changes of sea level (relative sea level – RSL) with respect to the land, while altimeters express more globally uniform changes (mean sea level – MSL) (Rovere, 2016). Moreover, the latest novelty in satellite measurements is gravimetry, which indirectly estimates the ocean water mass (barystatic contribution to global mean sea level (GMSL)) (Leuliette, 2015). A more analytical description of gravimetry data is given in section **2.1.4.**

Secondly, there are two types of mechanisms that contribute to the sea level change. The first one is eustatic change and the second one is isostatic rebound. The first one affects global sea level and the second one is mostly observed at regional scales. According to the Austrian geologist Edward Suess, sea level regression phases were caused by the storage of water in ice sheets on land combined with contraction of the ocean water due to decrease in temperature (Suess,1906). As a consequence, it can be deduced that eustatic changes are caused by changes in the water mass or volume. While mass changes happen with the addition or subtraction of water into the oceans and water redistribution due to wind stress and oceanic currents (Gill and Niller, 1973; Stammer *et al*., 2016), volume changes occur when variations in temperature and salinity take place. Increasing temperature leads to thermal expansion of the water, whereas decrease in salinity contracts the water. Furthermore, tectonic movements potentially affect the volume of an oceanic basin and therefore contribute to the eustatic sea level (Church *et al*., 2013). Interestingly, what makes mean sea level changes non-uniform globally is the variation of the

land water storage, either in liquid or solid state (ice), which contributes to the rise or fall of the Earth's crust, often referred to as isostatic rebound.

Sea level change is of major interest, to researchers, as well as to governments and communities, since it highly impacts the lives of millions of people living in coastal areas. Climate change and/or extreme climatic events are directly reflected on the sea level (Leuliette, 2015), a fact that has been demonstrated throughout geologic time. As stated in the 5th Assessment Report of the Intergovernmental Panel on Climate Change (IPCC), during the period 1901-2010 global sea level rise was estimated at 1.74 ± 0.18 mm/yr, with an accelerated mean rate of 3.2 ± 0.4 mm/ yr from 1993 to 2010.

In this thesis, one of the main processes that affect the water mass of a basin, and as a consequence its sea level, has been studied. The freshwater budget, in essence the hydrological cycle, is a delicate balance between water that is lost to the atmosphere, e.g. from heating or from strong cold winds, or is stored in land as ice, and water that returns to the same area through precipitation, river runoff, underground water, land ice melting *etc*. It can be understood as a dynamical equilibrium between ocean and atmosphere. In the eustatic sense, it impacts directly the salinity and temperature of the ocean, and as a consequence the stability of the water column and the general circulation (Stammer, 2008; Yin *et al*., 2009), but it also contributes to the isostatic component, as land ice is formed. In the last century, anthropogenic activities like river damming and irrigation, have greatly altered the land water reservoirs, and as a result the sea level changes as well as the hydrological cycle (Sahagian, 2000; Wada *et al*., 2010).

The study area, the Black Sea (Fig. 2), is a semi-enclosed basin, located between Turkey, Bulgaria, Ukraine and other countries, with a maximum depth of approximately 2200 m, and a volume of 5.3 x 10^5 km^3 (Özsöy and Ünlüata, 1997). It is connected with the Mediterranean Sea through the Turkish Straits System, Bosphorus, Marmara Sea and Dardanelles. The basic features that determine the freshwater budget of this basin, and consequently its water mass, include the atmospheric forcing (precipitation and evaporation), river discharges, and the exchange of water with the Mediterranean Sea through the Bosphorus Strait. Specifically the Danube river fluxes have been found to have a significant correlation with Black Sea's sea level (Özsöy *et al*., 1998), due to the fact that this river contributes about 50% to the total river runoff (Özsöy and Ünlüata, 1997). The Azores and Siberian high-pressure systems play an important role in the setup of the Black Sea's climatology (Staneva and Stanev, 1998). Evaporation in particular is influenced by the strong dry winds over Black Sea's cold waters, which are more prominent over the west side of the basin (Romanou *et al.,* 2010).

The challenging aspect of the estimation of the freshwater budget of the particular basin lies in the inconsistency of the atmospheric datasets, a fact frequently mentioned by the scientific community. Romanou et al. (2010), for example, compared a set of atmospheric data from different sources (including the ERA-Interim reanalysis dataset) to satellite retrieved data and reported that the ERA datasets had smaller values than the National Centers for

Environmental Prediction/National Center for Atmospheric Research (NCEP/NCAR) data. Staneva and Stanev (1998) also point out to the discrepancies for evaporation and precipitation between the available measurements. Finally, according to Volkov and Landerer (2015), ERA-Interim's precipitation and evaporation values are not of the same order as the estimates of Özsöy and Ünlüata (1997), possibly leading to the conclusion that there is an underestimation of precipitation and an overestimation of evaporation regarding ERA-Interim data. Estimates of the freshwater budget components after extensive research from different publications are presented in Table 1. In cases where no description of the date or the type of data is shown in Table 1, it is due to the lack of further information from the sources themselves or from research which was published in Russian.

The last component which significantly influences the water budget, and therefore the sea level of a quasi-enclosed basin such as the Black Sea, is the net flux through the Turkish Straits (Garrett, 1983; Candela *et al*., 1989; Özsöy *et al*., 1998; Johns and Sofianos, 2012). Regarding the composition of the flow layers in Bosphorus, since the freshwater inputs (rivers and precipitation) far exceed evaporation, the surface current is characterized by low salinity and thus leaves Black Sea, while the bottom current is saltier and denser, coming from the Mediterranean (Fig. 2). This being said, the Black Sea is considered as an estuarine basin, with fjord-type circulation induced by the exchange of water with Mediterranean through the Turkish Straits (Maderich & Konstantinov, 2002; Kara *et al.,* 2008). Estimates from the scientific literature regarding the volume fluxes of Bosphorus Strait are presented in Table 2.

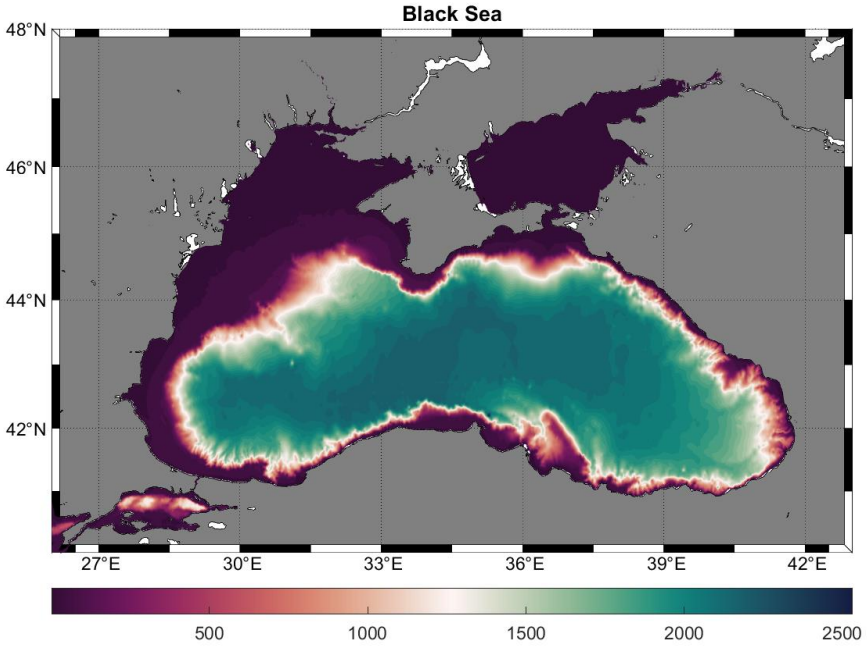

Figure 1. Bathymetry of the Black Sea. From General Bathymetric Chart of the Oceans (GEBCO).

Research in the past years has shown an accelerated rate of Black Sea's sea level. During the period 1960-1990 the Black Sea's sea level has risen by approximately 2 mm per year (Tsimplis and Baker, 2000). The sea level rise

assessment for the next eight years (1990-1998) regarding Black Sea was estimated at 27 mm per year (Stanev *et al*., 2000; Cazenave *et al*., 2002), which is a highly exacerbated rate. Another study by Allenbach et al. (2015) suggested that in the scenario of a 50 cm rise of the sea level, the surface of Black Sea's shores will decrease by half. For this reason, it is fundamental to inquire into both the sea level change and the mechanisms behind it.

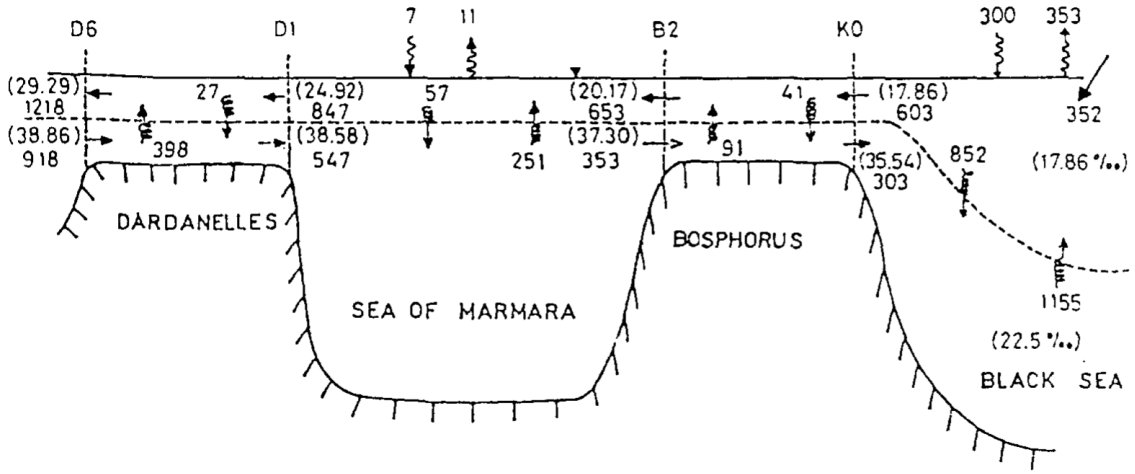

Figure 2. Schematic representation of the two-layer water flow regime in the Turkish Straits System. Volume fluxes are in km³/yr. Numbers in brackets represent average salinity. Taken from Beşiktepe et al., 1994.

This study aims to investigate the freshwater budget variability of Black Sea and its connection with the mean sea level, for a twelve year period (2003 to 2014). To achieve this result, an array of data has been analyzed. In section 2, a more detailed explanation about the data and the methods applied can be found. The results are demonstrated in section 3, and the discussion in section 4.

Table 1. Comparative values for atmospheric and riverine contribution to the Black Sea freshwater budget.

Authors	**Date**	**Type**	***E*** (m/yr)	***P*** (m/yr)	***R*** (m/yr)	***E-P*** (m/yr)	***E-P-R*** (m/yr)
Efimov & Timofeev, 1990						-0.37	
Simonov & Altman, 1991	1923-1985	Observ.	-0.84	0.5	0.72	-0.34	0.38
Ogüz et al., 1995	1923-1985	Observ.	-0.81	0.48	0.67	-0.33	0.34
Özsoy & Ünlüata , 1997	1987-1993	Observ.	-0.75	0.64	0.75	-0.11	0.64
Staneva & Stanev, 1998		Observ.	-0.83	0.69		-0.14	

Stanev et al., 2000	1992-1997	Observ.	-0.63	0.5	0.68	-0.13	0.55
Peneva et al., 2001							0.42
Schrum et al., 2001	1979-1993	Model	-0.7	0.45		-0.25	
Stanev & Peneva, 2002	1923-1997					-0.28	
Jaoshvili, 2002				0.5	0.74		
Kara et al., 2005	1979-1993	Model	-0.57	0.46	0.61	-0.11	0.5
Matsoukas et al., 2007	1984-2000	Model	-0.96				
Kara et al., 2008	1979-1993	Model	-0.57	0.47	0.61	-0.1	0.51
Romanou et al., 2010	1988-2005	Model	-0.65	0.47		-0.18	
Efimov et al., 2012	1958-2001	Model	-0.82	0.5	0.74	-0.32	0.42
Volkov & Landerer, 2015	1979-2014	Model	-0.83	0.51	0.64	-0.32	0.32

Table 2. Comparative values for the volume fluxes of the Bosphorus Strait.

Authors	Date	Type	Q_{in} (m/yr)	Q_{out} (m/yr)	Q_{net} (m/yr)
Özsoy et al., 1996	1991-1995	Observ.	0.23	-1.14	-0.9
Özsoy & Ünlüata , 1997	1987-1993	Observ.	0.64	-1.28	-0.64
Gregg & Özsoy, 2002	1994	Observ.	0.72	-1.09	-0.37
Jarosz et al., 2011	2008-2009	Observ.	0.64	-0.85	-0.21
Altiok et al., 2014	2003	Observ.	0.63	-0.74	-0.11
Maderich et al., 2015	1970-2009	Model	0.37	-0.91	-0.54
Altiok & Kayişoğlu, 2015	1999-2010	Observ.	0.54	-0.84	-0.3

2. Materials and Methods

2.1. Datasets

The freshwater budget variability of Black Sea and its relation to the mean sea level is examined for a twelve-year period (2003 to 2014) using updated and novel data sets. To assess the barystatic variability of the basin, a state-of-the-art dataset from NASA's Gravity Recovery and Climate Experiment mission (GRACE) has been utilized. Both climatology from the European Centre for Medium-Range Weather Forecasts (ECMWF) and hydrological data from Swedish Meteorological and Hydrological Institute (SMHI) have been employed to estimate the freshwater budget. The results from Stamatis Petalas novel 3-D model (Eastern Mediterranean Black Sea) have helped to close the remaining water balance, and lastly the altimetry measurements from EU Copernicus Marine Service Products have been used to investigate the relation of all the aforementioned data to the mean sea level.

2.1.1. Atmospheric forcing

Climatology from the European Centre for Medium-Range Weather Forecasts (ECMWF) was used in order to quantify the atmospheric processes which govern the water mass budget (evaporation-*E* and precipitation-*P*). ECMWF offers an array of products (e.g. Operational, Reanalysis and Atmospheric Composition). The selected product for this particular study was the ERA-INTERIM reanalysis for both *P* and *E*. ERA-INTERIM is a global atmospheric reanalysis forecast (Dee *et al*., 2011). For this thesis, *P* and *E* data were downloaded as NetCDF files using the ECMWF Web-API (see Appendix C), for the period of 2003-2014, with time selection of '00:00' and '12:00', 3-hour step selection '3'/'6'/'9'/'12', spatial resolution 0,125°×0,125° and Black Sea area coordinates 48 North, 26 West, 40 South and 43 East. Both evaporation and precipitation were provided in meters, after applying the center in time processing they were converted to kg m^{-2} s^{-1}, however, in order to compare the volumetric flow rates of all the water budget components they had to be converted to m^3 s^{-1}. The land-sea mask was downloaded with the same region coordinates.

2.1.2. River runoff

For the purpose of closing the fresh-water budget, river runoff data were downloaded for the study period (i.e 2003 to 2014) from the Swedish Meteorological and Hydrological Institute (SMHI), which derive from E-Hype v3.1.2 hydrological model (Hundecha *et al*., 2016). The data used for the Black Sea water mass budget included seven rivers discharging in the area of interest, utilizing the Representative Concentration Pathway RCP 2.6, and EC-Earth (Global Circulation Model) and RCA4 (Regional Climate Model) as model inputs/forcings. The seven rivers included Danube, Dniester, Dnjepr, Kuban, Red, Sakarya and Don. The riverine outflow was given in m^3 s^{-1}, the spatial resolution was of a median catchment size of 215 km^2, and the file was provided in XLS format.

2.1.3. Bosphorus upper (northeastern) side strait flow

Since not only the freshwater input/output contributes to the water mass budget of a basin, the inflow and outflow from the upper Bosphorus strait are required to aptly simulate the main mechanisms that contribute to the variability of the water volume/mass of the Black Sea. For this reason, upper and lower flow rates of the northeastern Bosphorus strait were used from Stamatis Petalas (personal communication) new Eastern Mediterranean Black Sea (EMBS2) 3-D model, which explicitly simulates the Turkish Straits exchanges, for the study period. The upper flow is considered as the water that exits the Black Sea, since its characteristic is low salinity (from now on Q_{out}). The lower flow is the water that is coming from the Marmara Sea into the Black Sea, which can be identified by its increased salinity (from now on Q_{in}). The volume was estimated in m^3 s^{-1} and the file was provided by Stamatis Petalas in XLS format. EMBS2 is the numerical simulation of the Eastern Mediterranean-Black Sea system for the period of 1985-2015, utilizing the hydrodynamic model of ocean circulation ROMS (Rutgers University). In order to simulate the dynamic of the Turkish Straits System in high frequency, a variable spacing grid with a horizontal resolution of 1-10 km was build, with 30 vertical levels in sigma coordinate system and a time step of 60 seconds. The boundary conditions at the air-sea interface were created according to ERA-Interim atmospheric data, and lastly the river runoff time series were constructed from SMHIs E-Hype v3.1.2 hydrological model data. It should be noted that the exchange provided by this model (EMBS2) compares well with previous independent studies (*e.g.* Maderich *et al.,* 2015), and is innovative given that it estimates the variability of the exchanges in a 30-year period.

2.1.4. GRACE

The Gravity Recovery and Climate Experiment (GRACE) mission was launched in March 2002, via the collaboration of National Aeronautics and Space Administration (NASA) and Deutsches Zentrum für Luft- und Raumfahrt (DLR) under the NASA's Earth System Science Pathfinder program, aiming to monitor the earth's gravity field (Watkins and Bettadpur, 2000; Tapley and Reigber, 2001). The mission utilizes two satellites with 220 km distance between them, at ~ 500 km altitude and 89.5° inclination, taking measurements with a monthly interval (Tapley *et al*., 2004). There are two available options regarding the GRACE solutions, Jet Propulsion Laboratory (JPL) solutions (Watkins *et al.,* 2015) and Goddard Space and Flight Center (GSFC) solutions (Luthcke *et al.,* 2013). The main difference between those datasets, except the different approach of the two laboratories to produce these results, is the usage of a Coastline Resolution Improvement (CRI) filter to prevent signal leakage from land to ocean (Wiese *et al.,* 2016), and the size of the mass concentration block (mascon). JPL provides bigger mascons with the application of the CRI filter, while GSFC has smaller mascons without a filter. The mass concentration blocks (mascons) used in this study were selected from JPL instead of GSFC, for the region of Black Sea, measuring the basin's mass in equivalent water height (cm) for the study period, and had been corrected in relation to isostatic changes with

Glacio Isostatic Adjustment (GIA). The definitive reason behind this choice was the trend of each time series. JPL mascons represented a rate of 0.21 cm/yr while GSFC mascons showed a change of 1.25 cm/yr (Loomis and Luthcke, 2017), which contradicts the existing literature. The region mascons option for Black Sea provided by Colorado Center for Astrodynamics Research (CCAR) consisted of 10 mascons. The file was in XLS format.

2.1.5. Altimetry Sea Level Anomaly

Daily SSALTO/DUACS Delayed-Time Level-4 sea surface height (SSH) with derived sea level anomaly (SLA) variables measured by multi-satellite altimetry observations over Black Sea from E.U Copernicus Marine Environment Monitoring Service (CMEMS) were employed to verify the trend depicted in the GRACE mascons data. The DUACS processing system is used on a variety of altimeter missions including Jason-3, Sentinel-3A, Cryosat-2, ENVISAT etc. The derivation of Black Sea SLAs map emerged from the Level-3 Sea Level observations and their optimal interpolation uniting measurements from different altimeter missions available. The spatial resolution of the SLA record was in 0,125° x 0,125° containing mean daily values. Data are available in netCDF format from http://marine.copernicus.eu/

2.2. Data Analysis/Methodology

In this section, the methods with which each distinctive set of data has been manipulated are presented and explained. As a whole, the analysis was conducted using mainly MATLAB® numerical computing environment, and Climate Data Operators (CDO), which is a tool that can be used in a Unix shell to perform several tasks related to scientific data analysis. All the codes developed and applied for the implementation of the thesis in question, are listed in two separate Appendices. All CDO codes are listed in **Appendix A**, and all MATLAB® routines in **Appendix B**.

2.2.1. Freshwater budget of the Black Sea

As a means to express the temporal variability of Black Sea's water budget, the following equation (1) was applied,

$$A\frac{d\eta}{dt} = Q_{in} + R + P - Q_{out} - E \quad (1)$$

where $d\eta$ is the term representing the changes of sea surface height in the given time step which is expressed through dt. The general concept is that the sum of the inputs and outputs of the basin's water volume is equivalent to the sea surface height of Black Sea divided by the time step, in which case is one month. As inputs are

considered the mechanisms that add to the total water balance (and therefore have a positive sign), namely the Q_{in}, R and P. The outputs are the mechanisms that subtract volume from the total water volume of the basin (negative sign), which are Q_{out} and E. The term A denotes the basin's surface area, which multiplied with the sea level change is a first order approximation for the rate of change of the water volume of the basin. The result of eq. (1) is expressed in $m^3\ s^{-1}$.

The area of Black Sea was calculated using the Land-Sea mask from ECMWF. The idea is that the area of Black Sea is equivalent with the double integral of the Land-Sea mask. This particular mask is a matrix with two values, 0 for land and 1 for the sea. The expression for the calculation of the total area of Black Sea is given by equation (2),

$$A = \iint mask \cos(\varphi) \frac{\pi}{180}\, dx\, dy \tag{2}$$

in which φ is the latitude for each grid cell converted into radians (e.g. in degrees from North to South 40°, 40.125°, 40.25° *etc*). Since the spatial resolution of ERA-INTERIM dataset is 0,125° x 0,125°, and 1° equals to 111120 m, it can be easily deduced that *dx* same as *dy*, since the grid is isotropic, is approximately equal to 13.890 m. The total surface of Black Sea basin was calculated to be approximately 4.6853 x 10^{11} m^2.

2.2.2. Definition of E_{net} and Q_{net}

Both the data of atmospheric forcing and river runoff together constitute the atmospheric and terrestrial branch of the freshwater budget E_{net} which is expressed via the following equation:

$$E_{net} = E - P - R \tag{3}$$

The net exchange rate at Bosphorus strait, i.e. the oceanic branch of the freshwater budget, is expressed by the difference between the incoming and outcoming waters (eq. 4):

$$Q_{net} = Q_{in} - Q_{out} \tag{4}$$

2.2.3. Atmospheric forcing center in time

E and *P* are accumulated fields from ECMWF's ERA-INTERIM forecast, which has the temporal option of a 3-hour step, as stated in paragraph **2.1.1**. For example, the precipitation with time 00:00 and step 3 hours, is the accumulated precipitation during this three-hour interval. As a means to center in time the given values for each

time step (3, 6, 9, 12), each quantity is divided by the duration of the time step in seconds (*e.g.* the accumulated precipitation of step 3 is divided by 3*3600 seconds).

2.2.4. Land-sea mask editing

To begin with, the necessity for a land-sea mask originates in the fact that the atmospheric forcing files contain information for the entire selected area. This means that there are extra data that are not useful, e.g. precipitation and evaporation over the surrounding land of Black Sea. Hence, the land-sea mask, containing zeros in the corresponding land grid cells and ones in the sea grid cells, is multiplied with the original forcing file to maintain solely the values that are of interest. The mask in question was visualized with Ncview program, and did not represent any particular problem, except from the fact that it maintained a portion from the Sea of Marmara. However, when visualized with MATLAB® software, the orientation was inverted, e.g. the north coordinates appeared in the south, the west coordinates in the east *etc.* Therefore, the first step was to flip the dimensions of the land-sea mask matrix and then proceed to modify the values which correspond to the Sea of Marmara. Consequently, the mask was multiplied with the original forcing files to mask out all atmospheric exchanges over land.

2.2.5. Averaging of daily data

Two different tools were used to average the daily *E, P* and *R* data, for the purpose of creating new monthly time series. After the completion of all ECMWF's atmospheric forcing fields center in time explained in paragraph **2.2.1**, the transition from daily 3-hour values to daily-mean and to monthly-mean time series was carried out with the aid of CDO operators. The final step was to generate a new time series for each year, averaging the values from all the grid cells of the netCDF file of the corresponding year, which was also accomplished with the CDO operators. The monthly averaging of the river runoff data was conducted with a routine written in MATLAB® programming language. Equally, the volumetric upper flow rate of Bosphorus strait was given as daily average values, and its conversion to monthly average was made with the aforementioned routine. Ultimately, with regard to Black Sea SLA files, the original format was daily average. Their conversion to monthly average, and the creation of a time series for the whole area of the basin was carried out with the CDO operators. Finally, a yearly averaging was applied for the extraction of a yearly rate of change for the basin's mass concentration written in MATLAB® programming language.

2.2.6. Interpolation of GRACE mascons

The convection when a time series is given in monthly values is that those values are centered in each month e.g. 15 January, 16 February *etc.* GRACE mascons data did not meet this standard, as the monthly values were positioned in different instants than the centre of each month. Another problem was the absence of some monthly values which needed to be filled. Therefore the mascons data were interpolated with simple linear interpolation, with a means to adjust every time series analyzed with the exact same time vector.

2.2.7. Trend and seasonality adjustment

As stated from Huang and Peng (2007), a time series trend is considered as the best fit straight line that expresses the tendency of the data throughout the whole studied period, which could be positive or negative. Another component of climatic data time series is seasonality. It is best represented by the periodic fluctuations of the data observed during approximately a 12 month period, reflecting the changes of seasons e.g. increased precipitation during winter season and decreased precipitation during summer. Both de-trending and de-seasonalizing constitute fundamental processes when analyzing non-linear and non-stationary time series, since they remove repetitive patterns and reveal the underlying motif. MATLAB® has the intrinsic function `detrend` which removes the linear trend from the selected data. The logic of the de-seasonalizing consists of removing the mean value of each month from the initial time series, e.g. mean value of all Januaries removed from each January value of the study period. The above-mentioned adjustments were performed when necessary.

2.2.8. Indirect estimation of steric component

According to Jordà and Gomis (2013), the fluctuations of the sea level height can be expressed by the following equation:

$$\frac{\partial \eta}{\partial t} = -\frac{1}{\rho_s}\int_{z=-H}^{z=\eta(t)} \frac{\partial \rho}{\partial t} dz + \frac{1}{\rho_s}\frac{\partial}{\partial t}\left(\frac{\delta m}{\delta A}\right) \quad (5)$$

where $\frac{\partial \eta}{\partial t}$ is the temporal variability of the sea level height, $\eta(t)$ is the free surface height, ρ_s is the surface density and ρ is the density of the water column, H is the depth, δm the mass of the water in the water column and lastly δA is an horizontal section. In eq. (5) the first term represents the steric component, and the second term indicates the mass component. The steric effect is linked with the changes in temperature T and salinity S of the water column. Increased temperature leads to thermal expansion of the water (thermosteric component), while a rising salinity brings compression of the water (halosteric component) (Jordà and Gomis, 2013). The above changes are

translated into fluctuations in the density of the seawater. In comparison with the available data, the previous equation can be interpreted as follows:

$$SLA = steric + mass\ (GRACE) \tag{6}$$

According to eq. (6), the subtraction of the mass component from the *SLA* data results in the steric component of the sea level height change, which was applied for the case of the Black Sea.

2.2.9. Cross correlation and running mean

To successfully locate a possible correlation and its time lag between time series, a cross correlation routine was used, which was kindly conceded from professor V. Zervakis. If x and y are two quantities, their correlation coefficient can be calculated by the division of their covariance with the product of their standard deviation, as showed in equation (7).

$$R = \frac{C(x,y)}{s_x\, s_y} = \frac{1}{N-1}\frac{\sum_{i=1}^{N}(x_i - \bar{x})(y_i - \overline{y})}{\sqrt{\sum_{i=1}^{N}(x_i - \bar{x})^2 \sum_{i=1}^{N}(y_i - \bar{y})^2}} \tag{7}$$

The above expression can be modified to time lagged cross correlation, which is shown in the equation below,

$$r(j) = \frac{1}{N-1}\frac{\sum_{i=1}^{N}(x_i - \bar{x})(y_{i+j} - \overline{y})}{\sqrt{\sum_{i=1}^{N}(x_i - \bar{x})^2 \sum_{i=1}^{N}(y_i - \bar{y})^2}} \tag{8}$$

where *r(j)* is the correlation of x and y quantities, with the time step of *j*. In reality, this is a measurement that demonstrates if x quantity leads y, and with which time difference. Furthermore, to evaluate the inter-annual variability of both branches of the freshwater budget, a running mean (routine was kindly conceded from professor V. Zervakis) was applied to the raw time series using a Hamming window, as it is one of the simplest low-pass filters in physical oceanography (Emery and Thomson, 2001). The Hamming window, which is a variation of the Hanning window, falls under the umbrella of the $\cos^a(x)$ window family (Harris, 1978). This particular window is expressed via the following equation for α= 0.54 and *N*=24:

$$w(n) = \alpha + (1-\alpha)\cos\left(\frac{2\pi}{N}\right), \qquad n = -\frac{N}{2}, \dots, \frac{N}{2} \tag{9}$$

3. Results

3.1. Freshwater budget of the Black Sea

The raw time series of the atmospheric and terrestrial branch (*E*, *P* and *R*) of the freshwater budget are shown in Fig. 4, while the exact same components plus their algebraic sum E_{net} are visualized in Fig. 5. The mean values for the atmospheric inputs and rivers contributing to the freshwater balance are $\bar{E} \cong$ -0.78 m yr^{-1}, $\bar{P} \cong$ 0.42 m yr^{-1} and $\bar{R} \cong$ 0.78 m yr^{-1}, while mean *E-P-R* ≅ 0.42 m yr^{-1}. All the components show great seasonal variability, which can be seen in Fig. 6. The results have shown that E_{net} is greatly influenced by the maxima of river runoff and evaporation, shaping its sign accordingly, and in a lower percentage by peaks of precipitation (Fig. 5, 6).

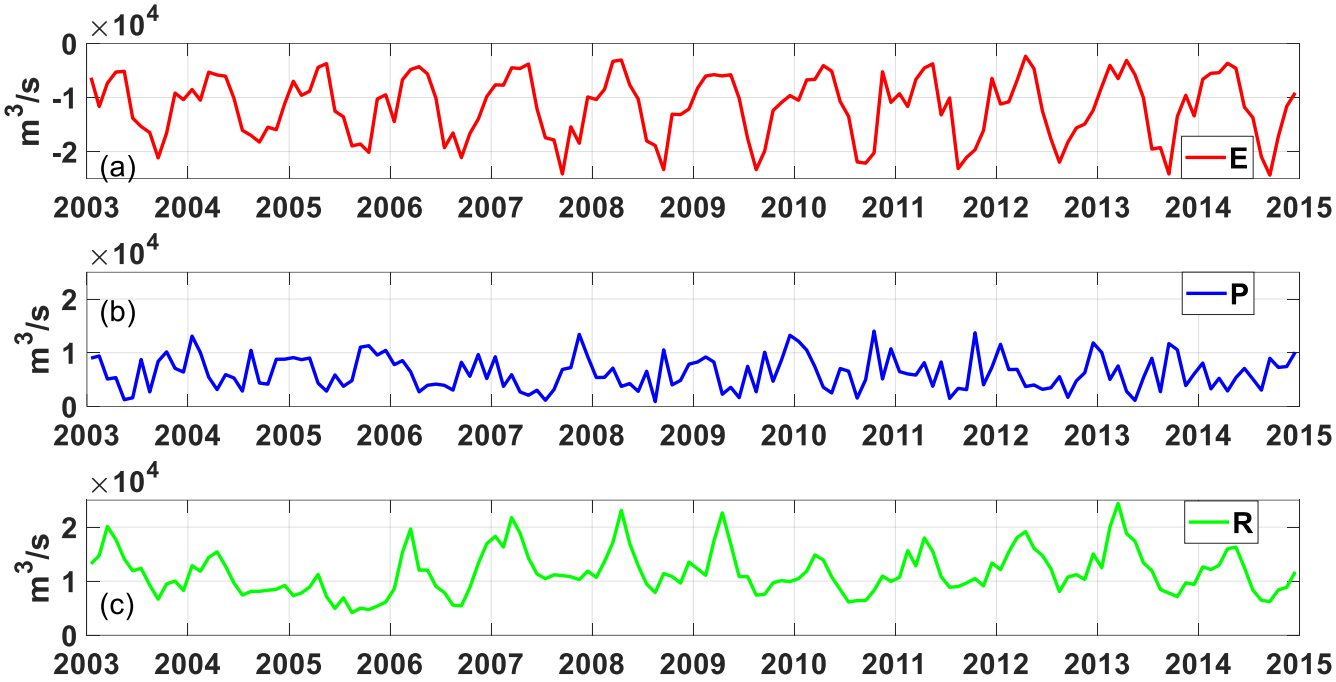

Figure 2. (a) Evaporation, (b) Precipitation and (c) River discharge original timeseries in m³/s.

Evaporation exhibits maxima during September and minima in April while precipitation shows higher values in December-January and lower values in May. Contrary to evaporation, river runoff peaks in April and decreases in August (Fig. 6). In inter-annual timescale, river runoff exhibits increase, as well as E_{net}, while on the contrary precipitation has a negative trend. Evaporation shows a stable trend throughout the study period (Fig. 7). The oceanic branch of the freshwater budget, expressed as Q_{in} and Q_{out}, with the algebraic sum Q_{net} is shown in Fig. 8.

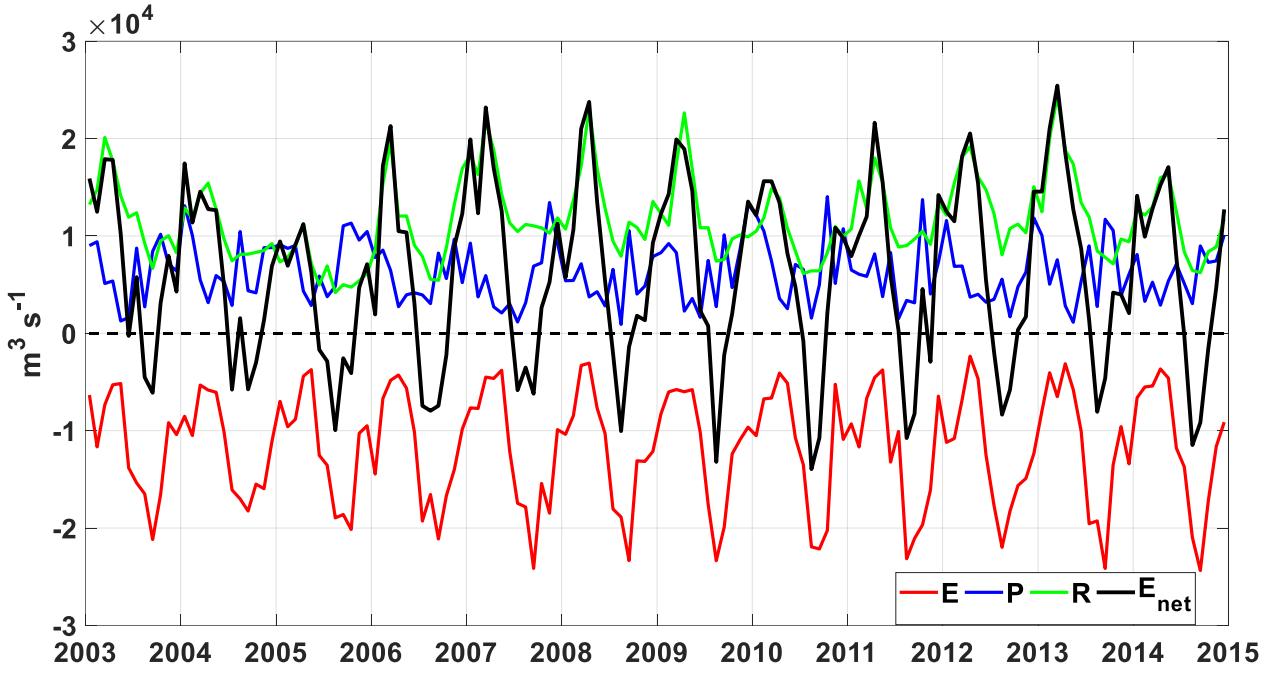

Figure 3. Evaporation, precipitation, river discharge and E_{net} original timeseries in m^3/s.

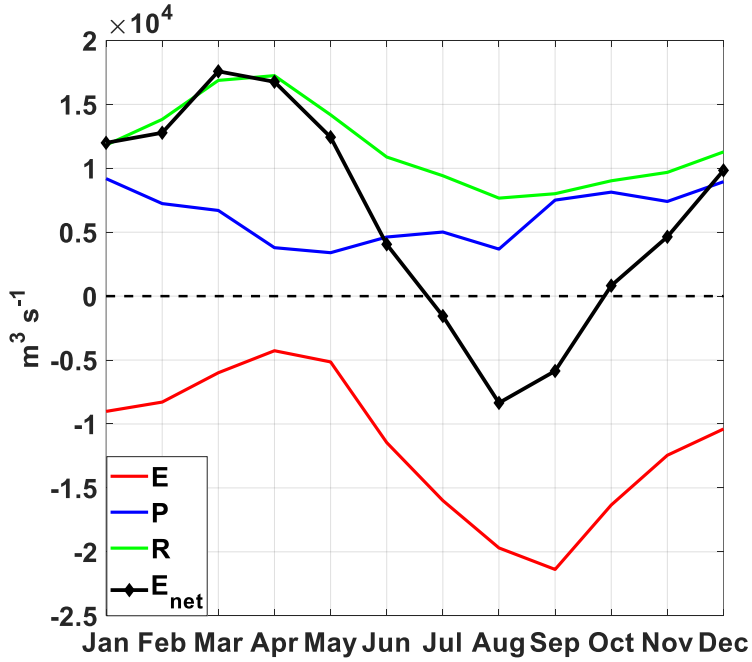

Figure 4. Seasonality of the atmospheric and terrestrial branch of the freshwater budget.

Mean values of Q_{in}, Q_{out} and Q_{net} are 0.35, -1.25 and -0.9 m/yr respectively. The net volume flux through the Bosphorus Strait is greatly influenced by the variability of Q_{in} and Q_{out}, and is mostly negative, except occasions in which Q_{out} dropped significantly while Q_{in} increased (Fig. 9).

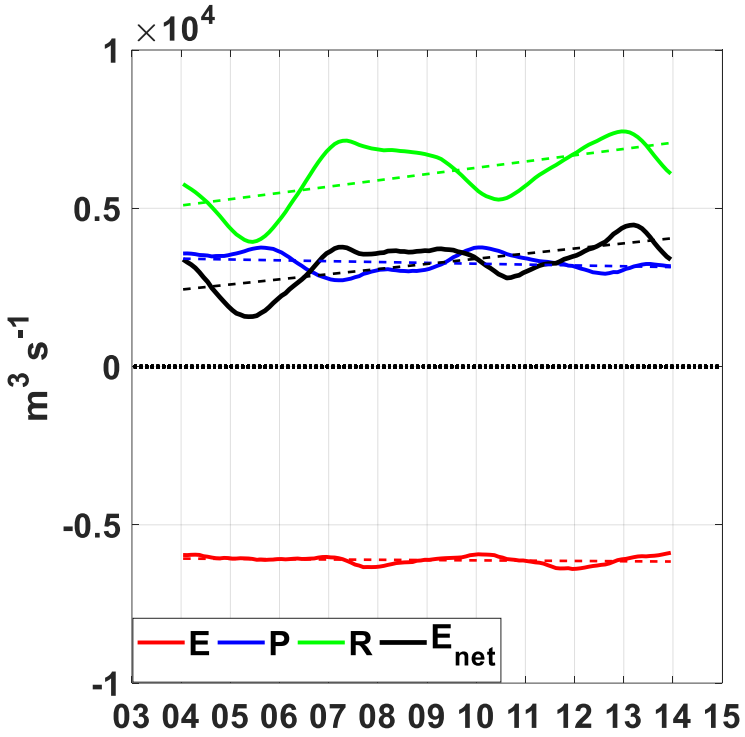

Figure 5. Inter-annual variability of the atmospheric and terrestrial branch of the freshwater budget, window length N=24.

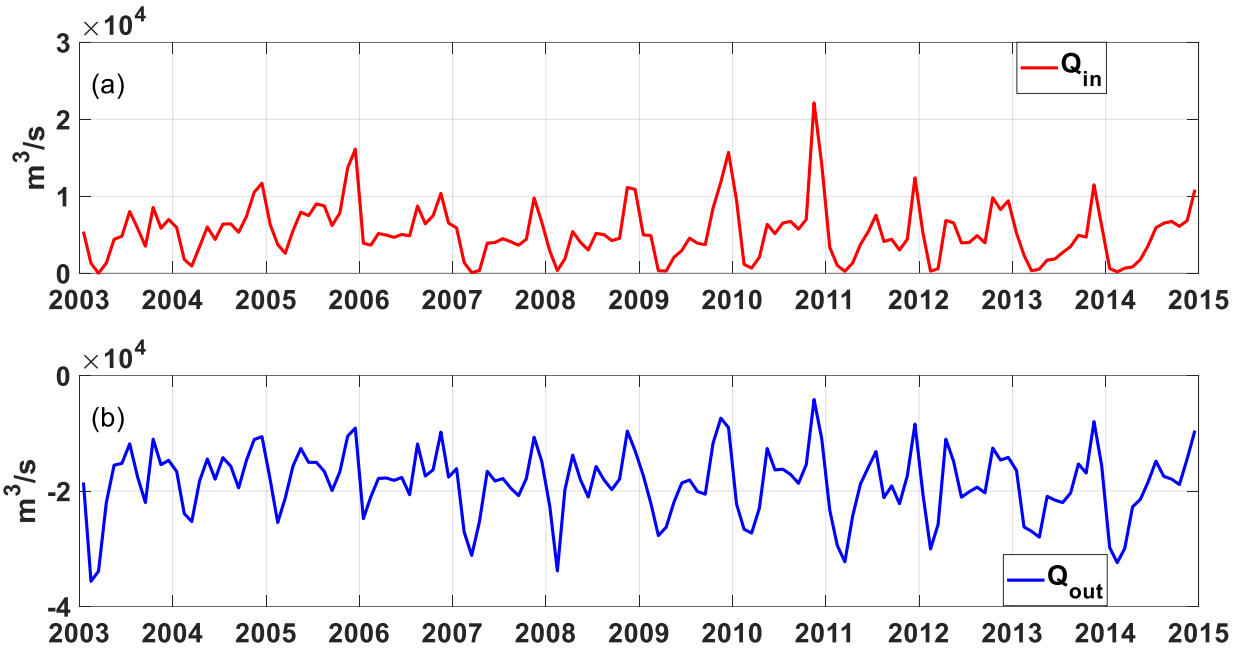

Figure 6. . (a) Q_{in} and (b) Q_{out} original timeseries in m³/s.

In annual timescale, Q_{net} is close to zero during November-December, when Q_{in} exhibits maxima, and its highest value coincides with the highest value of Q_{out} during February-March. Q_{in} and Q_{out} seem to have opposite phase, given that when one of the above quantities increases the other decreases and vice-versa (Fig. 10). In inter-annual timescale, the incoming water from the Mediterranean has a negative trend, while the out-flowing water from the Black Sea shows a positive trend (Fig. 11).

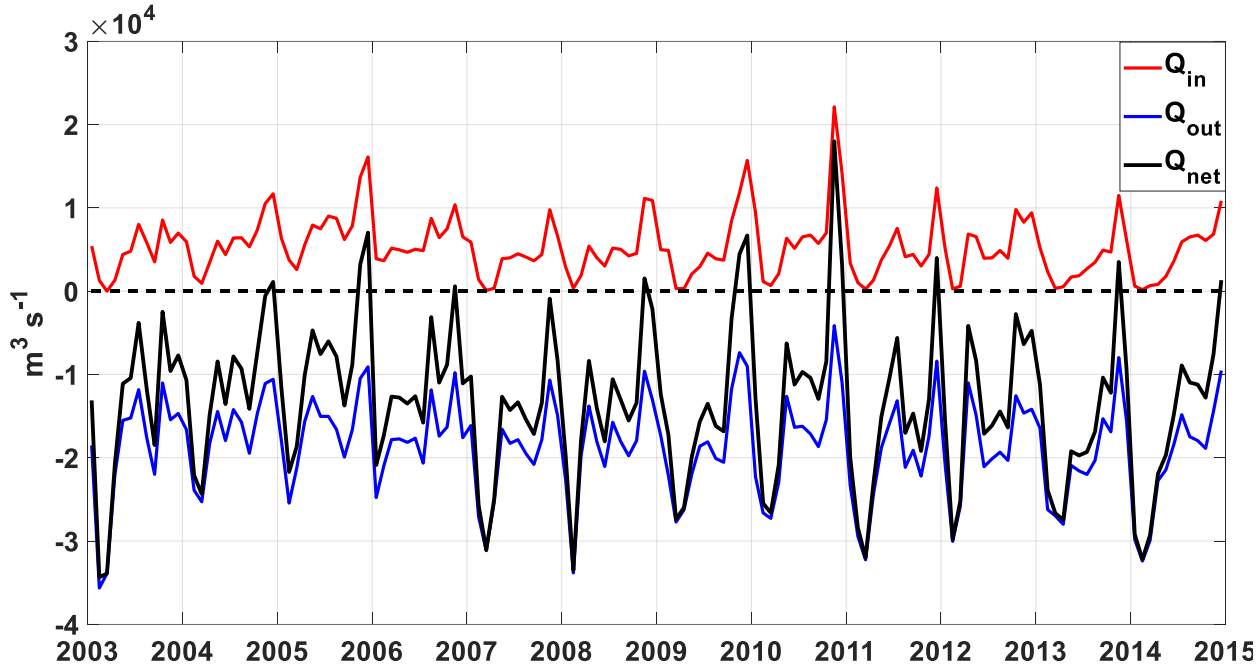

Figure 7. Q_{in}, Q_{out}, and Q_{net} original timeseries in m³/s.

Moreover, the net atmospheric and terrestrial branch E_{net} and the net oceanic branch Q_{net} along with the total freshwater budget are shown in Fig 12. Positive values for the total water budget are shaped by high E_{net} and low or positive Q_{net}, while negative are influenced by negative phases of E_{net} and positive or low Q_{net}.

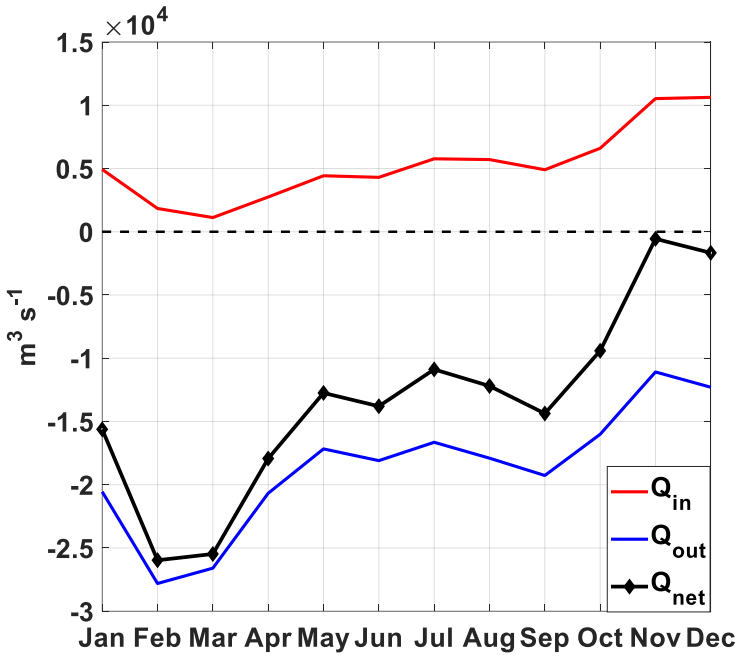

Figure 8. Seasonality of the oceanic branch of the freshwater budget.

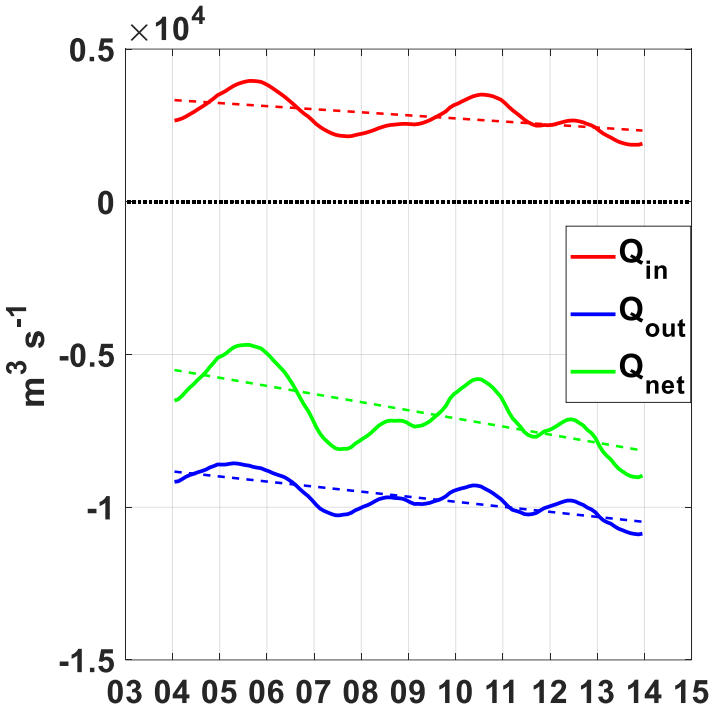

Figure 9. Inter-annual variability of the oceanic branch of the freshwater budget, window length N=24.

Two notable positive anomalies for the total water budget were observed in 2009 and 2010, where both E_{net} and Q_{net} had positive sign (Fig. 12), seem to have influenced the mass gain expressed by the GRACE data, as shown in Fig. 13.

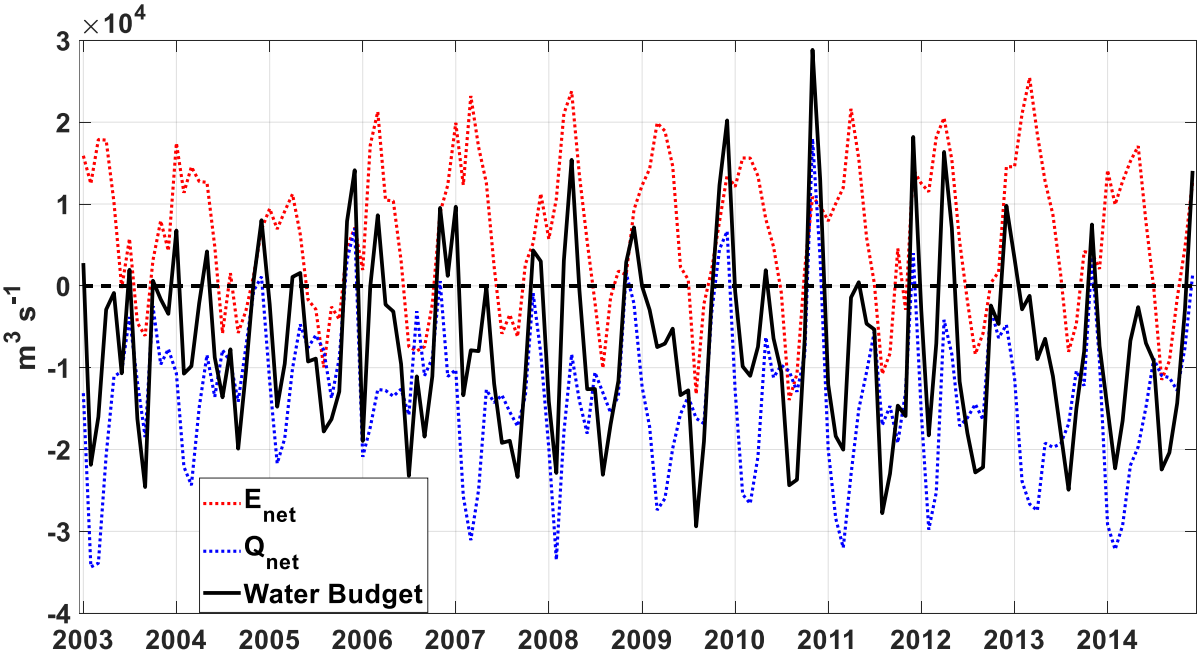

Figure 10. E_{net}, Q_{net} and freshwater budget in m³/s.

3.2. Water budget and water mass of Black Sea

The comparison of the freshwater budget with the temporal variability of the basin's water mass, which in essence is the visualization of eq. (1), is of great interest (Fig. 13), given that it illustrates the presence of a common phase between both quantities. This can be confirmed by the correlation coefficient value which is approximately 0.46. There are two notable positive anomalies in both measurements during late 2009-early 2010 and late 2010 which will be discussed in more detail in discussion and conclusions section. Furthermore, in Fig. 14 the time lagged cross correlation between the aforementioned quantities demonstrates that the variations in the freshwater budget are leading the variability of Black Sea's water mass by one month (for x=1 the correlation is ~ 0.44), while the cross correlation between E_{net} and Q_{net} showed maximum correlation (~ 0.43) at approximately two months (Fig. 15) implying that atmospheric and terrestrial forcing is followed by the Strait exchange response by an average of two months.

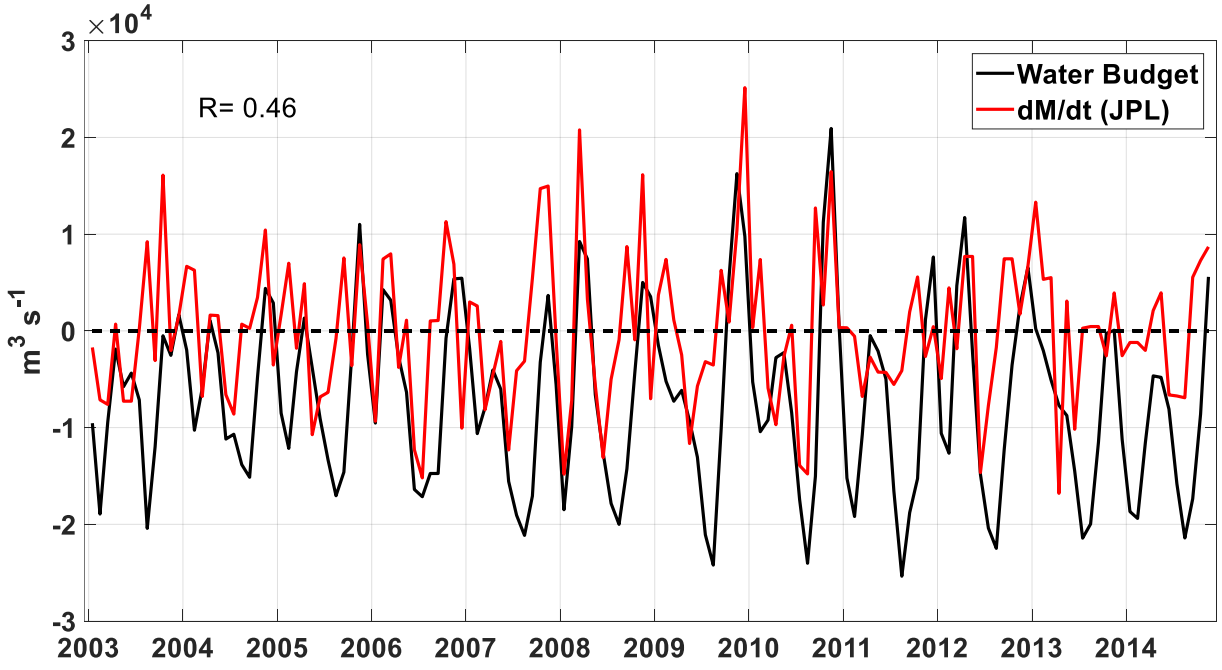

Figure 11. Illustration of the temporal variability of Black Sea's water mass and the total water budget in m³/s.

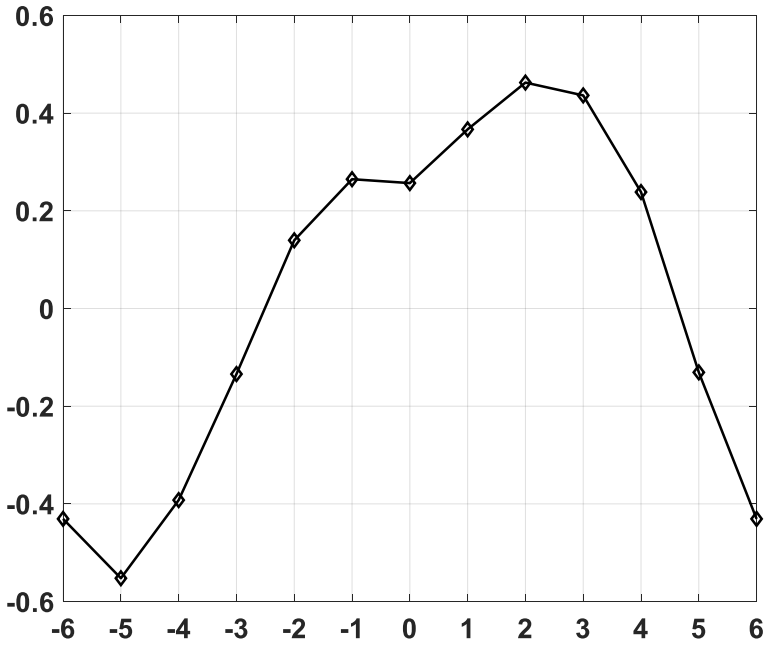

Figure 12. Time lagged cross-correlation E_{net} and Q_{net} with a 6 month time window.

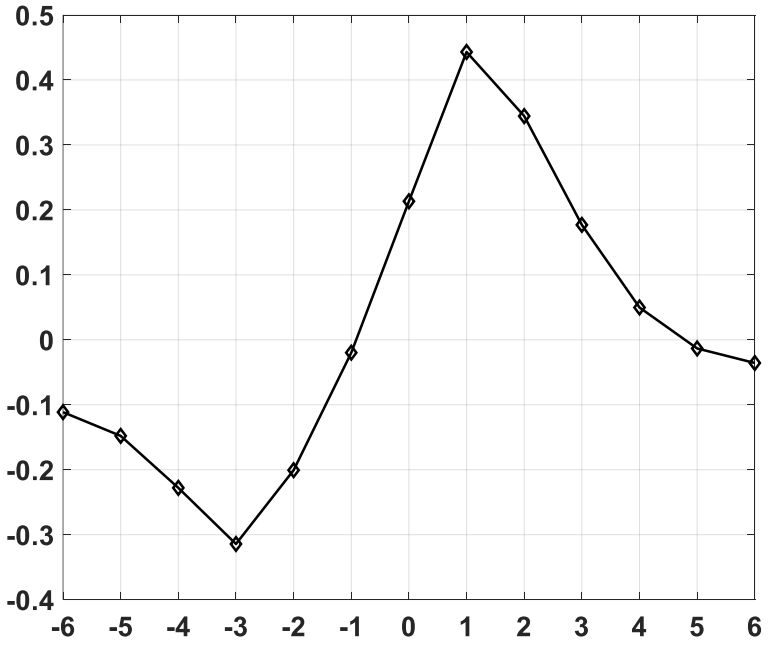

Figure 13. Time lagged cross-correlation between total water budget and mass variability with a 6 month time window.

3.3. Sea level anomalies comparison with GRACE mascons and trend estimation

Following, the connection between the water mass and the SLAs of Black Sea is represented in Fig. 16. The variability of GRACE water mass time series is verified by the same changes in the SLAs, a fact which is proved by

the correlation coefficient between these two quantities (r ~ 0.76) (Fig. 16a). Both time series show similar trends. Fig. 16b shows the monthly rate of change for both measurements. SLA presents a trend of 2.5 mm/yr while JPL mass concentration has an increase of 1.9 mm/yr. If we embrace the logic of eq. (6), an increase in the total sea level and the mass component, depicts that to compensate the overall change of the sea level, the leftover component, which is the steric, will correspond to a relatively small and positive trend.

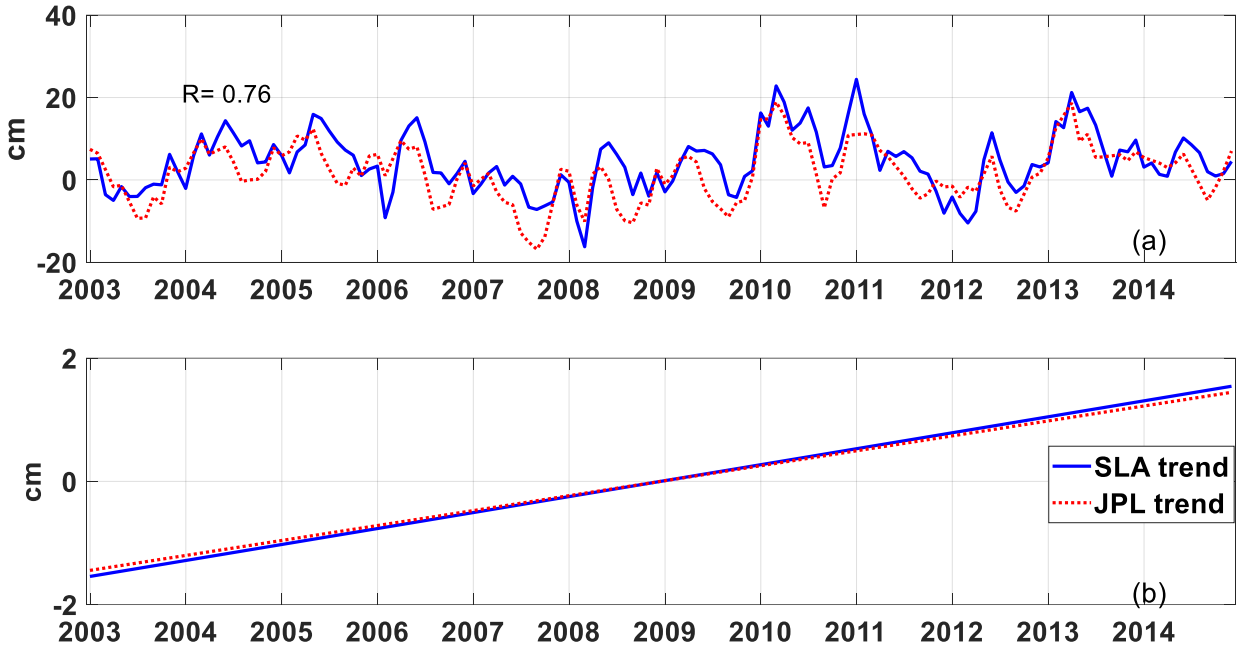

Figure 14. (a) Comparison between SLA (blue line) and mass component(red dotted line) variability. (b) SLA trend (blue) JPL-mass trend (red) (cm).

4. Discussion and conclusions

To summarize, the main objective of this thesis is the investigation of the freshwater budget of the Black Sea and its variability and its relation to the recorded mean sea level. Each dataset utilized to calculate the overall freshwater budget seems to correlate well with the mass and sea level fluctuations of Black Sea for the study period, despite the fact that the datasets were provided from independent sources. Initially, the correlation between water budget and mass variability is satisfactory provided that they constitute a mixture of estimates from independent origins. Realistically, it is nearly impossible to have complete accordance between datasets which do not originate from field measurements or at least the same source. As described in the introduction there are visible discrepancies between atmospheric datasets and therefore freshwater budget estimates, thanks to the combination of methods applied to calculate them. Studies in the past have used the products of reanalysis forecasts combined with parameters calculated via bulk formulas as well as field observations. Specifically about precipitation, Staneva and Stanev (1998) refer to a West-East gradient, with typical values of 0.3-0.5 m/yr and 1.8-2.5 m/yr respectively, which was attributed to local orography. Furthermore, the estimations of latent heat flux have great uncertainties, and as

a consequence evaporation, due to the scarcity of moisture flux data (Weare, 1989; Kent and Taylor, 1995; Gleckler and Weare, 1997). Concerning the mixture of data analyzed in this thesis, ERA-INTERIM estimates have their own errors since they are products of models. SHMI also utilizes atmospheric data from ERA-INTERIM as initial conditions in the hydrological models, and consequently the error in *R* values is increased. The same rationale applies for EMBS2 model, which uses both ERA-INTERIM and SHMI data as initial conditions to produce the water fluxes through Bosphorus Strait. GRACE data carry their own sources of error, since signal leakage from land to ocean exists (Watkins et al., 2015). More targeted efforts towards the improvement of the atmospheric forecast products and a meticulous comparison between evaporation and precipitation estimates would significantly contribute to the understanding of the water cycle. Nevertheless, the GRACE mascons data can very well explain the observed trend of Black Sea's sea level rise. The results of the mean sea level rise presented in this thesis are in accordance with Kubryakov et al. (2017) and Avsar et al. (2015). It should be noted that according to Kubryakov et al. (2017), the mean sea level rise of the Black Sea was found to be non-uniform spatially between 1993-2014, with an accelerated rate at coastal areas compared to the center of the basin. The water mass rise rate given in the results section is in agreement with Avsar et al. (2018) whose estimate was 2.3 ± 1.0 mm/yr for the period 2002-2017.

Moreover, all the components of the freshwater budget appear to be strongly influenced by seasonal variations, and in their turn greatly impact the net water flux of Bosphorus. In particular, there is strong correlation between maximum river discharge and outgoing flow at Bosphorus strait. Volkov and Landerer (2015) concluded that the combination of increased river discharge and reduced Q_{out} was responsible for the positive SLA anomalies observed in early 2010 and 2013. Considering the upper and lower layers of Bosphorus flux, the maximum Q_{in} during winter coincides with the lowest Q_{out} values. Jarosz et al. (2011a,b) explain that the reduction of the outgoing flow from Black to Marmara Sea can be influenced by strong winds. In fact, flow reversal (known as "Orkoz") of the upper layer of the upper part of the strait between October and November 2008 has been proved (Jarosz *et al.,* 2011b; Beşiktepe *et al.,* 1994; Özsoy *et al.,* 1998), but was not demonstrated by the results of this study.

The high positive anomalies of the water budget, possibly triggered by the combination of positive Q_{net} (late 2009-2010) and high E_{net} values (late 2009-early 2010, late 2012-early 2013), have very likely impacted the mass component of the Black Sea and by extension its sea level. This impact of the water budget to the mass and sea level can be validated by the positive time lagged cross correlation between the first two measurements. Tsimplis et al. (2004) attributes the positive sea level change to increased freshwater budget values, which is consistent with the results of this study.

Lastly, regarding the steric component of the mean sea level change, the deduction that springs from Fig. 16a is that in order to explain the proximity of both SLA and JPL positive trends, the steric trend is supposed to be very small and not significant to the SLA rise which also comes in accordance with the results of Tsimplis et al. (2004).

However, in a recent analysis Loomis and Luthcke (2017) examing the GRACE GSFC mascon solutions concluded that the steric trend of Black Sea for the period of 2005-2014 was negative. For this reason, a future assessment of the steric effect in the Black Sea would be a great improvement for the general understanding of the variability of the basin's mean sea level.

5. References

Allenbach K, Garonna I, Herold C, Monioudi I, Giuliani G, Lehmann A, Velegrakis AF, 2015. Black Sea beaches vulnerability to sea level rise. *Environmental Science & Policy* **46**: 95-109.

Altiok H, Aslan A, Övez S, Demirel N, Yüksek A, Kiratli N, Taş S, Müftüoğlu AE, Sur HI, Okuş E, 2014. Influence of the extreme conditions on the water quality and material exchange flux in the Strait of Instanbul. *Journal of Marine Systems* **139**: 204-216.

Altiok H, Kayişoğlu M, 2015. Seasonal and Interannual Variability of Water Exchange in the Strait of Instanbul. *Mediterranean Marine Science* **16** (3): 636-647.

Avsar NB, Jin S, Kutoglu SH, 2018. Recent Sea Level Changes in the Black Sea from satellite gravity and altimeter measurements. *The International Archives of the Photogrammetry, Remote Sensing and Spatial Information Sciences* **XLII-3/W4**: 83-85

Avsar NB, Kutoglu SH, Erol B, Jin S, 2015. Coastal Risk Analysis of the Black Sea under the Sea Level Rise. *FIG Working Week, From the Wisdom of the Ages to the Challenges of the Modern World,* 17-21 May, Sofia, Bulgaria.

Beşiktepe ŞT, Sur HI, Özsoy E, Latif MA, Oğuz T, Ünlüata Ü, 1994. The circulation and hydrography of the Marmara Sea. *Progress in Oceanography* **34**: 285-334.

Candela J, Winant CD, Bryden HL, 1989. Meteorologically forced subinertial flows through the Strait of Gibraltar. *Journal of Geophysical Research* **94** (C9): 12667-12679.

Cazenave A, Bonnefond P, Mercier F, Dominh K, Toumazou V, 2002. Sea level variations in the Mediterranean Sea and Black Sea from satellite altimetry and tide gauges. *Global and Planetary Change* **34** (1-2): 59-86.

Church JA, Clark PU, Cazenave A, Gregory JM, Jevjereva S, Levermann A, Merrifield MA, Milne GA, Nerem RS, Nunn PD, Payne AJ, Pfeffer WT, Stammer D, Unnikrishnan AS, 2013. Sea level change. In: Stocker TF, Qin D, Plattner GK *et*

al. (eds), *Assessment Report of the Intergovernmental Panel on Climate Change,* Cambridge University Press, Cambridge; New York, pp. 1137-1216.

Dee DP, Uppala SM, Simmons AJ, Berrisford P, Poli P, Kobayashi S, Andrae U, Balmaseda MA, Balsamo G, Bauer P, Bechtold P, Beljaars ACM, van de Berg L, Bidlot J, Bormann N, Delsol C, Dragani R, Fuentes M, Geer AJ, Haimberger L, Healy SB, Hersbach H, Hólm EV, Isaksen L, Kållberg P, Köhler M, Matricardi M, McNally AP, Monge-Sanz BM, Morcrette J-J, Park B-K, Peubey C, de Rosnay P, Tavolato C, Thépaut J-N, Vitart F, 2011. The ERA-Interim reanalysis: configuration and performance of the data assimilation system. *Quarterly Journal of the Royal Meteorological Society* **137**: 553–597.

Efimov VV, Belokopytov VN, Anisimov AE, 2012. Estimation of Water Balance Components in the Black Sea. *Russian Meteorology and Hydrology* **37** (11/12): 769-774.

Efimov VV, Timofeev A, 1990. Investigation of the Black Sea and Azov Sea heat balance. Ukrainian Academy of Science, Sevastopol, Ukraine.

Emery WJ, Thomson RE, 2001. Data Analysis Methods in Physical Oceanography. Second Edition. *Elsevier.* 654 pp.

Garrett CJR, 1983. Variable sea level and strait flows in the Mediterranean: A theoretical study of the response to meteorological forcing. *Oceanologica Acta* **6** (1): 79-87.

Gleckler PJ, Weare BC, 1997. Uncertainties in global ocean surface heat flux climatologies derived from ship observations. *Journal of Climate* **10**: 2764-2781.

Gill AE, Niller PP, 1973. The theory of the seasonal variability in the ocean. *Deep Sea Research and Oceanographic Abstracts* **20**: 141-177.

Gregg MC, Özsoy E, 2002. Flow, water mass changes, and hydraulics in the Bosphorus. *Journal of Geophysical Research* **107** (C3): 3016.

Harris FJ, 1978. On the Use of Windows for Harmonic Analysis with the Discrete Fourier Transform. *Proceedings of the IEEE* **66**: 51-83.

Huang N, Peng CK, 2007. On the trend, detrending, and variability of nonlinear and nonstationary time series. *Proceedings of the National Academy of Sciences* **104** (38): 14889-14894.

Hundecha Y, Arheimer B, Donnelly C, Pechlivanidis I, 2016. A regional parameter estimation scheme for a pan-European multi-basin model. *Journal of Hydrology: Regional Studies* **6**: 90-111.

Jaoshvili S, 2002. The rivers of the Black Sea. *European Environmental Agency* **58**, Technical report 71.

Jarosz E, Teague WJ, Book JW, Besiktepe S, 2011a. Observed volume fluxes in the Bosphorus Strait. *Geophysical Research Letters* **38**: L21608.

Jarosz E, Teague WJ, Book JW, Besiktepe S, 2011b. On flow variability in the Bosphorus Strait. *Journal of Geophysical Research* **116**: C08038.

Johns WE, Sofianos SS, 2012. Atmospherically forced exchange through the Bab el Mandeb Strait. *Journal of Physical Oceanography* **42:** 1143-1157.

Jordà G, Gomis D, 2013. On the interpretation of the steric and mass components of sea level variability: The case of the Mediterranean basin. *Journal of Geophysical Research: Oceans* **118**: 953-963.

Kara AB, Wallcraft AJ, Hurlburt HE, Stanev EV, 2008. Air-sea fluxes and river discharges in the Black Sea with a focus on the Danube and Bosphorus. *Journal of Marine Systems* **74**: 74-95.

Kara AB, Hurlburt HE, Wallcraft AJ, 2005. Black Sea Mixed Layer Sensitivity to Various Wind and Thermal Forcing Products on Climatological Time Scales. *Journal of Climate* **18**: 5266-5293.

Kent EC, Taylor PK, 1995. A comparison of heat flux estimates for the North Atlantic Ocean. *Journal of Physical Oceanography* **25**: 1530-1549.

Kopp RE, Hay CC, Little CM, Mitrovica JX, 2015. Geographic Variability of Sea-Level Change. *Current Climate Change Reports* **1** (3): 192-204.

Kubryakov AA, Stanichny SV, Volkov DL, 2017. Quantifying the impact of basin dynamics on the regional sea level rise in the Black Sea. *Ocean Science* **13**: 443-452.

Leuliette EW, 2015. The Balancing of the Sea-Level Budget. *Current Climate Change Reports* **1**: 185-191.

Leuliette EW, Nerem RS, Mitchum GT, 2004. Calibration of TOPEX/Poseidon and Jason Altimeter Data to Construct a Continuous Record of Mean Sea Level Change. *Marine Geodesy* **27** (1-2): 79-94.

Loomis BD, Luthcke SB, 2017. Mass evolution of Mediterranean, Black, Red, and Caspian Seas from GRACE and altimetry: accuracy assessment and solution calibration. *Journal of Geodesy* **91**: 195-206.

Luthcke SB, Sabaka TJ, Loomis BD, Arendt AA, McCarthy JJ, Camp J, 2013. Antartica, Greenland and Gulf of Alaska land-ice evolution from an iterated GRACE global mascon solution. *Journal of Glaciology* **59**(216): 613-631.

Maderich V, Ilyin Y, Lemeshko E, 2015. Seasonal and interannual variability of the water exchange in the Turkish Straits System estimated by modeling. *Mediterranean Marine Science* **16**(2): 444-459.

Maderich V, Konstantinov S, 2002. Seasonal Dynamics of the System Sea-Strait: Black Sea-Bosphorus Case Study. *Estuarine, Coastal and Shelf Science* **55**: 183-196.

Matsoukas C, Banks AC, Pavlakis KG, Hatzianastassiou N, Stackhouse PW, Vardavas I, 2007. Seasonal heat budgets of the Red and Black seas. *Journal of Geophysical Research* **112**: C10017.

Öguz T, Malanotte-Rizzoli P, Aubrey D, 1995. Wind and thermohaline circulation of the Black Sea driven by yearly mean climatological forcing. *Journal of Geophysical Research* **100** (C4): 6845-6863.

Özsoy E, Latif MA, Besiktepe ST, Cetin N, Gregg MC, Belokopytov V, Goryachkin Y, Diaconu V, 1998. The Bosphorus Strait: Exchange fluxes, currents, and sea level changes.In : *Ecosystem Modeling as a Management Tool for the Black Sea, NATO Science Series* **2**, *Environmental Security* **47**, edited by Ivanov L and Ogus T, pp. 1-27, Kluwer Academy, Dordrecht, Netherlands.

Özsoy E, Ünlüata Ü, 1997. Oceanography of the Black Sea: a review of some recent results. *Earth-Science Reviews* **42**: 231-272.

Özsoy E, Latif MA, Sur HI, Goryachkin Y, 1996. A review of the exchange flow regime and mixing in the Bosphorus Strait. *Bulletin de l'Institut océanographique* **17**: 187-204.

Peneva E, Stanev E, Belokopytov V, Le Traon PY, 2001. Water transport in the bosphorus straits estimated from hydro-meteorological and altimeter data: seasonal to decadal variability. *Journal of Marine Systems* **31**: 21-33.

Rhein M, Rintoul SR , Aoki S, Campos E, Chambers D, Feely RA, Gulev S, Johnson GC, Josey SA, Kostianoy A, Mauritzen C, Roemmich D, Talley LD, Wang F, 2013. Observations: Ocean. In: Climate Change 2013: The Physical Science Basis. Contribution of Working Group I to the Fifth Assessment Report of the Intergovernmental Panel on Climate Change [Stocker TF, Qin D, Plattner GK, Tignor M, Allen SK, Boschung J, Nauels A, Xia Y, Bex , Midgley PM (eds.)]. Cambridge University Press, Cambridge, United Kingdom and New York, NY, USA.

Romanou A, Tselioudis G, Zerefos CS, Clayson CA, Curry JA, Andersson A, 2010. Evaporation-Precipitation Variability over the Mediterranean and the Black Seas from Satellite and Reanalysis Estimates. *Journal of Climate* **23**: 5268-5287.

Rovere A, Stocchi P, Vacchi M, 2016. Eustatic and Relative Sea Level Changes. *Current Climate Change Reports* **2**: 221-231.

Sahagian D, 2000. Global physical effects of anthropogenic hydrological alterations: sea level and water redistribution. *Global and Planetary Change* **25** (1-2): 39-48.

Schrum C, Staneva J, Stanev E, Özsoy E, 2001. Air-sea exchange in the Black Sea estimated from atmospheric analysis for the period 1979-1993. *Journal of Marine Systems* **31**: 3-19.

Simonov AI, Altman EN, 1991. *Black Sea* Vol. 4, *Hydrometeorology and Hydrochemistry of the USSR Seas,* Gidrometeoizdat, 430 pp.

Stammer D, Cazenavev A, Ponte RM, Tamisiea ME, 2013. Causes for contemporary regional sea level changes. *Annual Review of Marine Science* **5**: 21-46.

Stammer D, 2008. Response of the global ocean to Greenland and Antartic ice melting. *Journal of Geophysical Research: Oceans,* C06022.

Staneva JV, Stanev EV, 1998. Oceanic response to atmospheric forcing derived from different climatic data sets. Intercomparison study for the Black Sea. *Oceanologica Acta* **21** (3): 393-417.

Stanev EV, Peneva EL, 2002. Regional sea level response to global climatic change: Black Sea examples. *Global Planetary Changes* **32**: 33-47.

Stanev EV, Le Traon PY, Peneva EL, 2000. Sea level variations and their dependency on meteorological and hydrological forcing: Analysis of altimeter and surface data for the Black Sea. *Journal of Geophysical Research: Oceans* **105** (C7): 17203-17216.

Suess E, 1906. The face of the earth. *Oxford: Clarendon Press.*

Tapley BD, Bettadpur S, Ries JC, Thompson PF, Watkins M, 2004. GRACE Measurements of Mass Variability in the Earth System. *Science* **305**: 503-505.

Tapley BD, Reigber C, 2001. The GRACE Mission: Status and future plans. *Eos Transactions American Geophysical Union* **82** (47): G41C-02.

Tsimplis MN, Josey SA, Rixen M, Stanev EV, 2004. On the forcing of sea level in the Black Sea. *Journal of Geophysical Research* **109**: C08015.

Tsimplis MN, Baker TF, 2000. Sea level drop in the Mediterranean Sea: An indicator of deep water salinity and temperature changes? *Geophysical Research Letters* **27** (12): 1731-1734.

Volkov DL, Landerer FW, 2015. Internal and external forcing of sea level variability in the Black Sea. *Climate Dynamics* **45**: 2633-2646.

Wada Y, van Beek LP, van Kempen CM, Reckman JWTM, Vasak S, Bierkens MFP, 2010. Global depletion of groundwater resources. *Geophysical Research Letters* **37** (20): L20402.

Watkins M, Wiese DN, Yuan DN, Boening C, Landerer FW, 2015. Improved methods for observing Earth's time variable mass distribution with GRACE using spherical cap mascons. *Journal of Geophysical Research: Solid Earth* **120**: 2648-2671.

Watkins M, Bettadpur S, 2000. The GRACE mission: challenges of using micron-level satellite-to-satellite ranging to measure the Earth's gravity field. *Proceedings of the International Symposium on Space Dynamics*, Biarritz, France, Centre National d'Etudes Spatiales (CNES).

Weare BC, 1989. Uncertainties in estimates of surface heat fluxes derived from marine reports over the tropical and sub-tropical oceans. *Tellus* **41A**: 357-370.

Wiese DN, Landerer FW, Watkins MM, 2016. Quantifying and reducing leakage errors in the JPL RL05M GRACE mascon solution. *Water Resources Research* **52**(9): 7490-7502.

Yin JJ, Schlesinger ME, Stouffer RJ, 2009. Model projections of rapid sea-level rise on the northeast coast of the United States. *Nature Geoscience* **2**: 262-266.

Appendix A – CDO

1. Evaporation and Precipitation

- *Daily Average*

```
time cdo  -v daymean bs_e_acc_2003.nc d_e2003.nc
time cdo  -v daymean bs_e_acc_2004.nc d_e2004.nc
time cdo  -v daymean bs_e_acc_2005.nc d_e2005.nc
time cdo  -v daymean bs_e_acc_2006.nc d_e2006.nc
time cdo  -v daymean bs_e_acc_2007.nc d_e2007.nc
time cdo  -v daymean bs_e_acc_2008.nc d_e2008.nc
time cdo  -v daymean bs_e_acc_2009.nc d_e2009.nc
time cdo  -v daymean bs_e_acc_2010.nc d_e2010.nc
time cdo  -v daymean bs_e_acc_2011.nc d_e2011.nc
time cdo  -v daymean bs_e_acc_2012.nc d_e2012.nc
time cdo  -v daymean bs_e_acc_2013.nc d_e2013.nc
time cdo  -v daymean bs_e_acc_2014.nc d_e2014.nc

time cdo  -v daymean bs_p_acc_2003.nc d_p2003.nc
time cdo  -v daymean bs_p_acc_2004.nc d_p2004.nc
time cdo  -v daymean bs_p_acc_2005.nc d_p2005.nc
time cdo  -v daymean bs_p_acc_2006.nc d_p2006.nc
time cdo  -v daymean bs_p_acc_2007.nc d_p2007.nc
time cdo  -v daymean bs_p_acc_2008.nc d_p2008.nc
time cdo  -v daymean bs_p_acc_2009.nc d_p2009.nc
time cdo  -v daymean bs_p_acc_2010.nc d_p2010.nc
time cdo  -v daymean bs_p_acc_2011.nc d_p2011.nc
time cdo  -v daymean bs_p_acc_2012.nc d_p2012.nc
time cdo  -v daymean bs_p_acc_2013.nc d_p2013.nc
time cdo  -v daymean bs_p_acc_2014.nc d_p2014.nc
```

- *Monthly Average*

```
time cdo -v monmean d_e2003.nc m_e2003.nc
time cdo -v monmean d_e2004.nc m_e2004.nc
time cdo -v monmean d_e2005.nc m_e2005.nc
time cdo -v monmean d_e2006.nc m_e2006.nc
time cdo -v monmean d_e2007.nc m_e2007.nc
time cdo -v monmean d_e2008.nc m_e2008.nc
time cdo -v monmean d_e2009.nc m_e2009.nc
time cdo -v monmean d_e2010.nc m_e2010.nc
time cdo -v monmean d_e2011.nc m_e2011.nc
time cdo -v monmean d_e2012.nc m_e2012.nc
time cdo -v monmean d_e2013.nc m_e2013.nc
time cdo -v monmean d_e2014.nc m_e2014.nc

time cdo -v monmean d_p2003.nc m_p2003.nc
time cdo -v monmean d_p2004.nc m_p2004.nc
```

time cdo -v monmean d_p2005.nc m_p2005.nc
time cdo -v monmean d_p2006.nc m_p2006.nc
time cdo -v monmean d_p2007.nc m_p2007.nc
time cdo -v monmean d_p2008.nc m_p2008.nc
time cdo -v monmean d_p2009.nc m_p2009.nc
time cdo -v monmean d_p2010.nc m_p2010.nc
time cdo -v monmean d_p2011.nc m_p2011.nc
time cdo -v monmean d_p2012.nc m_p2012.nc
time cdo -v monmean d_p2013.nc m_p2013.nc
time cdo -v monmean d_p2014.nc m_p2014.nc

- *Field Mean*

time cdo -v fldmean m_e2003.nc mf_e2003.nc
time cdo -v fldmean m_e2004.nc mf_e2004.nc
time cdo -v fldmean m_e2005.nc mf_e2005.nc
time cdo -v fldmean m_e2006.nc mf_e2006.nc
time cdo -v fldmean m_e2007.nc mf_e2007.nc
time cdo -v fldmean m_e2008.nc mf_e2008.nc
time cdo -v fldmean m_e2009.nc mf_e2009.nc
time cdo -v fldmean m_e2010.nc mf_e2010.nc
time cdo -v fldmean m_e2011.nc mf_e2011.nc
time cdo -v fldmean m_e2012.nc mf_e2012.nc
time cdo -v fldmean m_e2013.nc mf_e2013.nc
time cdo -v fldmean m_e2014.nc mf_e2014.nc

time cdo -v fldmean m_p2003.nc mf_p2003.nc
time cdo -v fldmean m_p2004.nc mf_p2004.nc
time cdo -v fldmean m_p2005.nc mf_p2005.nc
time cdo -v fldmean m_p2006.nc mf_p2006.nc
time cdo -v fldmean m_p2007.nc mf_p2007.nc
time cdo -v fldmean m_p2008.nc mf_p2008.nc
time cdo -v fldmean m_p2009.nc mf_p2009.nc
time cdo -v fldmean m_p2010.nc mf_p2010.nc
time cdo -v fldmean m_p2011.nc mf_p2011.nc
time cdo -v fldmean m_p2012.nc mf_p2012.nc
time cdo -v fldmean m_p2013.nc mf_p2013.nc
time cdo -v fldmean m_p2014.nc mf_p2014.nc

2. *Sea Level Anomaly*

- *Monthly Average*

time –v cdo monmean black_sea_sla.nc bs_m_sla.nc

- *Field Mean*

time –v cdo fldmean bs_m_sla.nc bs_fm_sla.nc

Appendix B – MATLAB

Calculation of Black Sea area

```
function [area]=calc_bs_area

dx=13890;
dy=dx;

lat=nc_varget('bs_e_acc_2002.nc','lat');

load correct_mask.mat

deg2rad=pi/180;

% area=sum(sum(mask2.*dx.*dy.*cos(lat(:,1)*deg2rad)));
area=sum(sum(mask2.*dx.*dy.*cos(lat(:,1)*deg2rad)));

end
```

Conversion of serial year to date

```
function [num] = ConvertSerialYearToDate( y )
  year = floor(y);
  partialYear = mod(y,1);
  date0 = datenum(num2str(year),'yyyy');
  date1 = datenum(num2str(year+1),'yyyy');
  daysInYear = date1 - date0;
  num = date0 + partialYear .* daysInYear;
end
```

Interpolation of GRACE mascons

```
mscn_sol=mscn_sol+datenum(2002,1,1,0,0,0);
JPL=JPL(8:140);
JPL_dt=mscn_sol(8:140);
JPL_int=interp1(JPL_dt,JPL,mtdan);
JPLm3s=((JPL_int.*area)./(30*24*3600))./100;
```

Monthly averaging

```
function [monthly,mtvec]=daily2mon(data,tvec,startyear,endyear)
%data=catchment
%tic;

yrind=endyear+1;
yrdif=yrind-startyear;
```

```
for i=endyear:-1:startyear;
    d{yrind-i,1}=find(tvec >= datenum(i,1,1,0,0,0) & tvec <=
datenum(i,12,31,0,0,0));
end

if length(size(data)) == 2;

    for i=1:yrdif;
        data_y{(yrdif+1)-i,1}=data(d{i},:);
        tvec_years{(yrdif+1)-i,1}=tvec(d{i,1});
    end

    for i=1:yrdif;
        data_m{i,1}=month_temp_avg(data_y{i,1});
        tvec_m{i,1}=month_temp_avg(tvec_years{i,1});
    end

elseif length(size(data)) == 3;

    for i=1:yrdif;
        data_y{(yrdif+1)-i,1}=data(d{i},:,:);
        tvec_years{(yrdif+1)-i,1}=tvec(d{i,1});
    end

    for i=1:yrdif;
        data_m{i,1}=month_temp_avg(data_y{i,1});
        tvec_m{i,1}=month_temp_avg(tvec_years{i,1});
    end

elseif length(size(data)) == 4;

    for i=1:yrdif;
        data_y{(yrdif+1)-i,1}=data(d{i},:,:,:);
        tvec_years{(yrdif+1)-i,1}=tvec(d{i,1});
    end

    for i=1:yrdif;
        data_m{i,1}=month_temp_avg(data_y{i,1});
        tvec_m{i,1}=month_temp_avg(tvec_years{i,1});
    end

end

monthly=cat(1,data_m{1:end,1});
mtvec=cat(1,tvec_m{1:end,1});

%toc;

End




function [mta]=month_temp_avg(data)
```

```
if size(data,1) == 366;

    mta(1,:)=squeeze(trapz(data(1:31,:)))/30.;
    mta(2,:)=squeeze(trapz(data(32:60,:)))/28.;
    mta(3,:)=squeeze(trapz(data(61:91,:)))/30.;
    mta(4,:)=squeeze(trapz(data(92:121,:)))/29.;
    mta(5,:)=squeeze(trapz(data(122:152,:)))/30.;
    mta(6,:)=squeeze(trapz(data(153:182,:)))/29.;
    mta(7,:)=squeeze(trapz(data(183:213,:)))/30.;
    mta(8,:)=squeeze(trapz(data(214:244,:)))/30.;
    mta(9,:)=squeeze(trapz(data(245:274,:)))/29.;
    mta(10,:)=squeeze(trapz(data(275:305,:)))/30.;
    mta(11,:)=squeeze(trapz(data(306:335,:)))/29.;
    mta(12,:)=squeeze(trapz(data(336:366,:)))/30.;

elseif size(data,1) == 365;

    mta(1,:)=squeeze(trapz(data(1:31,:)))/30.;
    mta(2,:)=squeeze(trapz(data(32:59,:)))/27.;
    mta(3,:)=squeeze(trapz(data(60:90,:)))/30.;
    mta(4,:)=squeeze(trapz(data(91:120,:)))/29.;
    mta(5,:)=squeeze(trapz(data(121:151,:)))/30.;
    mta(6,:)=squeeze(trapz(data(152:181,:)))/29.;
    mta(7,:)=squeeze(trapz(data(182:212,:)))/30.;
    mta(8,:)=squeeze(trapz(data(213:243,:)))/30.;
    mta(9,:)=squeeze(trapz(data(244:273,:)))/29.;
    mta(10,:)=squeeze(trapz(data(274:304,:)))/30.;
    mta(11,:)=squeeze(trapz(data(305:334,:)))/29.;
    mta(12,:)=squeeze(trapz(data(335:365,:)))/30.;



elseif size(data,1) == 152;

    mta(1,:)=squeeze(trapz(data(1:31,:)))/30.;
    mta(2,:)=squeeze(trapz(data(32:60,:)))/28.;
    mta(3,:)=squeeze(trapz(data(61:91,:)))/30.;
    mta(4,:)=squeeze(trapz(data(92:121,:)))/29.;
    mta(5,:)=squeeze(trapz(data(122:152,:)))/30.;


end
```

De-seasonalize

```
function [ sst ] = seasonality( data, timevector )
%Deseason Removes seasonality
%
%%%%%%%%%%%%%%%%%%%%%%%%%%%%%%%%%%%%%%%%%%%%%%%%%%%%%%%% Create seasonal indices
y=data;
%yy=detrend(y);
s=12;
T=length(y);
```

```
sidx=cell(s,1);

for i=1:s;
    sidx{i,1}=i:s:T;
end

%%%%%%%%%%%%%%%%%%%%%%%%%%%%%%%%%%%%%%%%%%%%%%%% Apply a stable seasonal filter

sst=cellfun(@(x) mean(y(x)),sidx);

%%%%%%%%%%%%%%%%%%%%%%%% Put smoothed values back into a vector of length N
%nc = floor(T/s); % no. complete years
%rm = mod(T,s); % no. extra months
%sst = [repmat(sst,nc,1);sst(1:rm)];

%%%%%%%%%%%%%%%%%%%%%%%%%%%%%%%%%%%% Center the seasonal estimate (additive)
sBar = mean(sst); % for centering
%sst = sst-sBar;

%%%%%%%%%%%%%%%%%%%%%%%%%%%%%%%%%%%%%%%%%%%%%%%%%%%%%%%%%%%%%%%% Deseasonalize the series

%deseason = y - sst;
mon=[1:12]';

%figure;
%subplot(2,1,1)
%plot(timevector, data,'r','LineWidth',1.4)
%ylabel('m^3 s^-^1','FontWeight','Bold','FontSize',14)
%datetick('x','yyyy');grid on;
%subplot(2,1,2)
%plot(mon,sst,'b','LineWidth',1.4)
%xlim=([1 12]);
%ylabel('m^3 s^-^1','FontWeight','Bold','FontSize',14)
%grid on;
end
```

General script

```
prec=importdata('prec.txt');

for i=1:size(prec);
mprec{i,1}=squeeze(nc_varget(prec{i,:},'rain'));
end
rain = cell2mat(mprec);

precipitation1=(rain./1000).*area;

Riv=mred+msak+mvolg+mkub+mdnjep+mdniest+mdan;

tvme=importdata('mon_e.txt');

for i=1:size(tvme);
me{i,1}=squeeze(nc_varget(tvme{i,:},'evap'));
end

E=cell2mat(me);
```

```
E=E(1:161);
Evaporation1=(E./1000).*area; % kg m^-2 s^-1 to m^3 s^-1

%%% Import SLA %%%

mon_sla=squeeze(nc_varget('fld_bs_sla.nc','sla'));
mon_sla_dt=squeeze(nc_varget('fld_bs_sla.nc','time'));
base=datenum(1950,1,1,0,0,0);
mon_sladt=mon_sla_dt+base;
msla=mon_sla.*100;

%%% Import Bosphorus Flow %%%

Q_upper_levelm3s=-Q_upper_levelm3s; % all in m3s
Qout=Q_upper_levelm3s;
Q_lower_levelm3s=-Q_lower_levelm3s;
Qin=Q_lower_levelm3s;
Qnet=-Q_netm3s;
Qalt_dt=[datenum(2003,01,01,12,0,0):datenum(2014,12,31,12,0,0)]';

[m_qin,mon_qaltdt]=daily2mon(Qin,Qalt_dt,2003,2014);
[m_qout,mon_qaltdt]=daily2mon(Qout,Qalt_dt,2003,2014);
[m_qnet,mon_qaltdt]=daily2mon(Qnet,Qalt_dt,2003,2014);


enet=evaporation1-precipitation1-Riv(1:144);
qnet=m_qin-abs(m_qout);
FWB=m_qin-abs(m_qout)-abs(evaporation1)+precipitation1+Riv(1:144);
dMJPL = diff(JPLm3s);


for i=1:143;
    meanfwb(i,1)=mean(FWB(i:i+1));
end

for i=1:143;
    meandt(i,1)=mean(mtdan(i:i+1));
end

Rr=corrcoef(meanfwb,dMJPL);

h=1;
for i=1:12:161;

    kak(h,1)=datenum(mon_sladt(i));
    h=h+1;
end

figure;
subplot(3,1,1)
plot(mtdan(1:144),evaporation1,'r','LineWidth',2.5)
str1=['(a)'];
T1 = text(datenum(2003,2,15,0,0,0),-19000, str1);
set(T1, 'fontsize', 22, 'verticalalignment', 'top', 'horizontalalignment',
'left')
ylabel('m^3/s','FontSize',22,'FontWeight','Bold')
```

```
legend({'E'},'FontSize',22,'FontWeight','Bold')
datetick('x','yyyy');grid on;
ax=gca;
ax.YLim=([-2.5*10^4 0]);
set(ax,'FontSize',22,'FontWeight','Bold')
subplot(3,1,2)
plot(mtdan(1:144),precipitation1,'b','LineWidth',2.5)
str2=['(b)'];
T2 = text(datenum(2003,2,15,0,0,0),21500, str2);
set(T2, 'fontsize', 22, 'verticalalignment', 'top', 'horizontalalignment',
'left')
ylabel('m^3/s','FontSize',22,'FontWeight','Bold')
legend({'P'},'FontSize',22,'FontWeight','Bold')
datetick('x','yyyy');grid on;
ax=gca;
ax.YLim=([0 2.5*10^4]);
set(ax,'FontSize',22,'FontWeight','Bold')
subplot(3,1,3)
plot(mtdan(1:144),Riv(1:144),'g','LineWidth',2.5)
str3=['(c)'];
T3 = text(datenum(2003,2,15,0,0,0),9500, str3);
set(T3, 'fontsize', 22, 'verticalalignment', 'top', 'horizontalalignment',
'left')
ylabel('m^3/s','FontSize',22,'FontWeight','Bold')
legend({'R'},'FontSize',22,'FontWeight','Bold')
datetick('x','yyyy');grid on;
ax=gca;
ax.YLim=([0 2.5*10^4]);
set(ax,'FontSize',22,'FontWeight','Bold')


figure;
subplot(2,1,1)
plot(mon_qaltdt,m_qin,'r','LineWidth',2.5)
str1=['(a)'];
T1 = text(datenum(2003,2,15,0,0,0),27000, str1);
set(T1, 'fontsize', 22, 'verticalalignment', 'top', 'horizontalalignment',
'left')
ylabel('m^3/s','FontSize',22,'FontWeight','Bold')
legend({'Q_i_n'},'FontSize',22,'FontWeight','Bold')
datetick('x','yyyy');grid on;
ax=gca;
%ax.YLim=([-2.5*10^4 0]);
set(ax,'FontSize',22,'FontWeight','Bold')
subplot(2,1,2)
plot(mon_qaltdt,m_qout,'b','LineWidth',2.5)
str2=['(b)'];
T2 = text(datenum(2003,2,15,0,0,0),-4000, str2);
set(T2, 'fontsize', 22, 'verticalalignment', 'top', 'horizontalalignment',
'left')
ylabel('m^3/s','FontSize',22,'FontWeight','Bold')
legend({'Q_o_u_t'},'FontSize',22,'FontWeight','Bold')
datetick('x','yyyy');grid on;
ax=gca;
%ax.YLim=([0 2.5*10^4]);
set(ax,'FontSize',22,'FontWeight','Bold')
```

```
figure; %subplot(2,1,1)
plot(mtdan(1:144),evaporation1,'r','LineWidth',2.5)
hold on
plot(mtdan(1:144),precipitation1,'b','LineWidth',2.5)
hold on
plot(mtdan(1:144),Riv(1:144),'g','LineWidth',2.5)
hold on
plot(mtdan(1:144),-enet,'k-','LineWidth',3)
hold on
plot(mtdan(1:144),zeros(length(qnet)),'k--','LineWidth',2)
datetick('x','yyyy');grid on;
ylabel('m^3 s^-^1','FontSize',22,'FontWeight','Bold')
legend({'E','P','R','E_n_e_t'},'FontSize',22,'FontWeight','Bold')
set(gca,'FontSize',22,'FontWeight','Bold')

figure; %subplot(2,1,1)
plot(mon_qaltdt,m_qin,'r','LineWidth',2.5)
hold on
plot(mon_qaltdt,m_qout,'b','LineWidth',2.5)
hold on
plot(mon_qaltdt,qnet,'k','LineWidth',3)
hold on
plot(mon_qaltdt,zeros(length(qnet)),'k--','LineWidth',2)
datetick('x','yyyy');grid on;
ylabel('m^3 s^-^1','FontSize',22,'FontWeight','Bold')
legend({'Q_i_n','Q_o_u_t','Q_n_e_t'},'FontSize',22,'FontWeight','Bold')
set(gca,'FontSize',22,'FontWeight','Bold')

mon=[1:12]';
[ sE ] = seasonality( evaporation1, mtdan(1:144) );
[ sP ] = seasonality( precipitation1, mtdan(1:144) );
[ sR ] = seasonality( Riv(1:144), mtdan(1:144) );
[ senet ] = seasonality( enet, mtdan(1:144) );
[ sqin ] = seasonality( m_qin, mon_qaltdt );
[ sqout ] = seasonality( m_qout, mon_qaltdt );
[ sqnet ] = seasonality( qnet, mon_qaltdt );


figure; %subplot(2,1,1)
plot(mon,sE,'r','LineWidth',2.5)
hold on
plot(mon,sP,'b','LineWidth',2.5)
hold on
plot(mon,sR,'g','LineWidth',2.5)
hold on
plot(mon,-senet,'kd-','MarkerSize',5,'LineWidth',3)
hold on
plot(mon,zeros(length(sR),1),'k--','LineWidth',2)
ax=gca;
ax.XLim=([1 12]);
ax.XTick=mon;
ax.XTickLabel=({'Jan','Feb','Mar','Apr','May','Jun','Jul','Aug','Sep','Oct','N
ov','Dec'});
set(ax,'FontSize',22,'FontWeight','Bold')
grid on;
ylabel('m^3 s^-^1','FontSize',22,'FontWeight','Bold')
```

```
legend({'E','P','R','E_n_e_t'},'FontSize',22,'FontWeight','Bold')

figure;plot(mon,sqin,'r','LineWidth',2.5)
hold on
plot(mon,sqout,'b','LineWidth',2.5)
hold on
plot(mon,sqnet,'kd-','LineWidth',3)
hold on
plot(mon,zeros(length(sqnet),1),'k--','LineWidth',2)
ax=gca;
ax.XLim=([1 12]);
ax.XTick=mon;
ax.XTickLabel=({'Jan','Feb','Mar','Apr','May','Jun','Jul','Aug','Sep','Oct','N
ov','Dec'});
set(ax,'FontSize',22,'FontWeight','Bold')
grid on;
ylabel('m^3 s^-^1','FontSize',22,'FontWeight','Bold')
legend({'Q_i_n','Q_o_u_t','Q_n_e_t'},'FontSize',22,'FontWeight','Bold')

[eH] = runningmeanw(evaporation1, 24, '@hamming');
[pH] = runningmeanw(precipitation1, 24, '@hamming');
[rH] = runningmeanw(Riv(1:144), 24, '@hamming');
[enH] = runningmeanw(enet, 24, '@hamming');
[qiH] = runningmeanw(m_qin, 24, '@hamming');
[qoH] = runningmeanw(m_qout, 24, '@hamming');
[qnH] = runningmeanw(qnet, 24, '@hamming');

eH1=eH(13:132);
pH1=pH(13:132);
rH1=rH(13:132);
enH1=enH(13:132);
eHdt=mtdan(13:132);

eHc=polyfit(eHdt,eH1,1);
eHf=polyval(eHc,eHdt);
pHc=polyfit(eHdt,pH1,1);
pHf=polyval(pHc,eHdt);
rHc=polyfit(eHdt,rH1,1);
rHf=polyval(rHc,eHdt);
enHc=polyfit(eHdt,enH1,1);
enHf=polyval(enHc,eHdt);

figure; %subplot(2,1,1)
plot(mtdan(1:144),eH,'r','LineWidth',2.5)
hold on
plot(mtdan(1:144),pH,'b','LineWidth',2.5)
hold on
plot(mtdan(1:144),rH,'g','LineWidth',2.5)
hold on
plot(mtdan(1:144),-enH,'k-','LineWidth',3)
hold on
plot(eHdt,eHf,'r--','LineWidth',1.7)
hold on
plot(eHdt,pHf,'b--','LineWidth',1.7)
hold on
plot(eHdt,rHf,'g--','LineWidth',1.7)
```

```
hold on
plot(eHdt,-enHf,'k--','LineWidth',1.7)
hold on
plot(mtdan(1:144),zeros(length(qnet)),'k:','LineWidth',2)
datetick('x','yy');grid on;
ylabel('m^3 s^-^1','FontSize',22,'FontWeight','Bold')
%title({'Low-passed time series, N=24'},'FontSize',22,'FontWeight','Bold')
legend({'E','P','R','E_n_e_t'},'FontSize',22,'FontWeight','Bold')
set(gca,'FontSize',22,'FontWeight','Bold')

qiH1=qiH(13:132);
qoH1=qoH(13:132);
qnH1=qnH(13:132);
qHdt=mon_qaltdt(13:132);

qiHc=polyfit(qHdt,qiH1,1);
qiHf=polyval(qiHc,qHdt);
qoHc=polyfit(qHdt,qoH1,1);
qoHf=polyval(qoHc,qHdt);
qnHc=polyfit(qHdt,qnH1,1);
qnHf=polyval(qnHc,qHdt);



figure; %subplot(2,1,1)
plot(mon_qaltdt,qiH,'r','LineWidth',2.5)
hold on
plot(mon_qaltdt,qoH,'b','LineWidth',2.5)
hold on
plot(mon_qaltdt,qnH,'g','LineWidth',2.5)
hold on
plot(qHdt,qiHf,'r--','LineWidth',1.7)
hold on
plot(qHdt,qoHf,'b--','LineWidth',1.7)
hold on
plot(qHdt,qnHf,'g--','LineWidth',1.7)
hold on
plot(mon_qaltdt,zeros(length(qnet)),'k:','LineWidth',2)
datetick('x','yy');grid on;
ylabel('m^3 s^-^1','FontSize',22,'FontWeight','Bold')
%title({'Low-passed time series, N=24'},'FontSize',22,'FontWeight','Bold')
legend({'Q_i_n','Q_o_u_t','Q_n_e_t'},'FontSize',22,'FontWeight','Bold')
%ax.XTick=[-1.2*10^4 -1*10^4 -0.8*10^4 -0.6*10^4 -0.4*10^4 -0.2*10^4 0
0.2*10^4 0.4*10^4];
ax=gca;
%ax.GridLineStyle = '-.'
ax.YAxis.Exponent = 4;
set(ax,'FontSize',22,'FontWeight','Bold')

[ja]=correl(enet,qnet,6);
xx=[-6:6]';
figure;plot(xx,ja,'kd-','LineWidth',2,'MarkerSize',8)
grid on;
ax=gca;
set(ax,'FontSize',22,'FontWeight','Bold')
ax.XTick=xx;
```

```
ax.XLim=([-6 6]);
%title('Time lagged cross-correlation E_n_e_t - Q_n_e_t,
N=6','FontSize',22,'FontWeight','Bold')

[je]=correl(FWB,JPLm3s,6)
xx=[-6:6]';
figure;plot(xx,je,'kd-','LineWidth',2,'MarkerSize',8)
grid on;
ax=gca;
set(ax,'FontSize',22,'FontWeight','Bold')
ax.XTick=xx;
ax.XLim=([-6 6]);
%title('Time lagged cross-correlation WB - JPL (m^3/s),
N=6','FontSize',22,'FontWeight','Bold')


Rr1=corrcoef(meanfwb,dMJPL);
figure;plot(meandt,meanfwb,'k-','LineWidth',2.5)
hold on
plot(meandt,dMJPL,'r-','LineWidth',2.5)
hold on
plot(meandt,zeros(length(meanfwb)),'k--','LineWidth',2)
ylabel('m^3 s^-^1','FontSize',22,'FontWeight','Bold')
legend({'Water Budget','dM/dt (JPL)'},'FontSize',22,'FontWeight','Bold')
disp(Rr1(1,2));
rr=round(Rr1,2);
str=['R= ',num2str(rr(1,2))]
T = text(datenum(2004,3,15,0,0,0),25000, str);
set(T, 'fontsize', 22, 'verticalalignment', 'top', 'horizontalalignment',
'left');
datetick('x','yyyy');grid on;
ax=gca;
set(ax,'FontSize',22,'FontWeight','Bold')
ax.XTick=kak;

m1=mean(msla(1:144));
m2=mean(JPL_int);
dm1=msla(1:144)-m1;
dm2=JPL_int-m2;

c1=polyfit(mon_sladt(1:144),dm1,1); %sla slope
c2=polyfit(mtdan(1:144),dm2,1); %jpl slope


f1=polyval(c1,mon_sladt(1:144));
f2=polyval(c2,mtdan(1:144));
figure;
subplot(2,1,1)
plot(mon_sladt(1:144),msla(1:144),'b-','LineWidth',1.3)
hold on
plot(mtdan(1:144),JPL_int,'r:','LineWidth',1.3)
ylabel('cm','FontSize',14,'FontWeight','Bold')
datetick('x','yyyy');grid on;
ax=gca;
ax.XTick=kak;
R = corrcoef(msla(1:144),JPL_int);
```

```
disp(R(1,2));
str=['R= ',num2str(R(1,2))];
T = text(datenum(2004,1,1,0,0,0),25, str);
set(T, 'fontsize', 14, 'verticalalignment', 'top', 'horizontalalignment',
'left');
str4=['(a)'];
T4 = text(datenum(2013,12,1,0,0,0),-10, str4);
set(T4, 'fontsize', 14, 'verticalalignment', 'top', 'horizontalalignment',
'left');
subplot(2,1,2)
plot(mtdan(1:144),f1,'b-','LineWidth',1.3)
hold on
plot(mtdan(1:144),f2,'r:','LineWidth',1.3)
legend({'SLA trend','JPL trend'},'FontSize',14,'FontWeight','Bold')
ax=gca;
datetick('x','yyyy');grid on;
ax.XTick=kak;
%ax.XLim=([2003 2014]);
%yr=[2003:2014]';
%ax.XTick=yr;
%grid on;
str5=['(b)'];
T5 = text(datenum(2013,12,1,0,0,0),-1.5, str5);
set(T5, 'fontsize', 14, 'verticalalignment', 'top', 'horizontalalignment',
'left');
%
```

Appendix C – API

```
#!/usr/bin/env python
from ecmwfapi import ECMWFDataServer

server = ECMWFDataServer()
server.retrieve({
   "class": "ei",
   "dataset": "interim",
   "expver": "1",
   "stream": "oper",
   "type": "fc",
   "levtype": "sfc",
   "param": "182.128/228.128",
   "date": "2003-01-01/to/2003-12-31",
   "time": "00/12",
   "step": "3/6/9/12",
   "grid": "0.125/0.125",
   "area":"48/26/40/43",
   "format":"netcdf",
   "target": "bs_e_p_2003.nc"
})
```